Mechanistic Insights into Iron-Catalyzed Allenic C–H Functionalization

by

Philip Nicholas Palermo

Bachelor of Science in Chemistry, University of Rochester, 2020

Submitted to the Graduate Faculty of the

Dietrich School of Arts and Sciences in partial fulfillment

of the requirements for the degree of

Master of Science

University of Pittsburgh

2023

UNIVERSITY OF PITTSBURGH

DIETRICH SCHOOL OF ARTS AND SCIENCES

This thesis was presented

by

Philip Nicholas Palermo

It was defended on

March 30, 2023

and approved by

Yiming Wang, Assistant Professor, Department of Chemistry

Wesley Transue, Assistant Professor, Department of Chemistry

Kay Brummond, Professor, Department of Chemsitry

Thesis Advisor: Yiming Wang, Department of Chemistry

Mechanistic Insights into Iron-Catalyzed Allenic C–H Functionalization

Philip Nicholas Palermo, MS

University of Pittsburgh, 2023

The mechanism for the iron-catalyzed C–H functionalization of simple monosubstituted allenes is investigated. In this report, we determined that the mechanism of this transformation involves a deprotonation causing the organoiron species to transform from a datively bound η^2-allene complex to a neutral η^1-propargyliron complex. This iron species acts as a nucleophile for *in-situ* generated electrophiles, performing a S_E2' type reaction resulting in a disubstituted allene. Herein, we additionally discuss the subtle differences in ligand design and the ramifications on various reaction yields through analysis of electronic properties and x-ray structure.

Table of Contents

List of Tables

List of Figures

Preface

I have had an excellent and memorable time during these years in the group and am thankful to all those who have helped me, both in and out of work, achieve all that I have. I wish to express my most sincere thanks to my supervisor, Professor Yiming Wang. I am grateful for all of his support and mentorship through everything. I would like to thank my committee members: Professor Kay Brummond and Professor Wesley Transue for their help and guidance. I express my sincere thanks to the former postdoc of our group, Dr. Yidong Wang and fellow graduate student Austin Durham for their contributions to the group's chemistry and their guidance on my research as well as all graduate students who worked concurrently in the group with me.

This work was supported by a grant from the National Institutes of Health- R35GM142945.

1.0 Introduction

Cyclopentadienyl iron species have been a cornerstone of organometallic chemistry since the discovery of ferrocene.[1] As Earth's most abundant transition metal, iron represents a highly attractive foundation for catalytic transformations. Monocyclopentadienyl iron complexes, referred to as piano stool or half-sandwich complexes, were conceived of shortly afterwards and applied towards various stoichiometric transformations[2-7] and catalytic applications due to its stability, relative non-toxicity, and its ease of characterization.[8-11] These traits are in part due to the η^5-cyclopentadiene ligand (Cp) and its unique and attractive properties. Cp strongly binds to the iron center and, as it infrequently slips into η^3 and η^1 configurations, it renders these sites unavailable for coordination which leads to greater reaction selectivity. The Cp ligand lends itself to various derivatives through inexpensive starting materials which, when complexated, can occupy larger portions of the coordination sphere as a spectator ligand while allowing for modulation of the core by steric and electronic effects.[12-15]

It has been observed that modified cyclopentadienyl, organometallic species express different stereoelectronic properties affected by their respective substituents[16-19]. These properties have been taken advantage of in order to improve catalytic viability, affect enantio- and diastereoselectivity, tune electromagnetic responses, and otherwise stabilize the new organometallic compound. With five membered rings, the possibilities for symmetric and asymmetric decoration are vast. Thus, understanding how slight differences in substitution affect the chemical properties of the Cp ligand can be crucial in predicting which variant may be of use in a future application. This communication seeks to explore the mechanism of a previously reported transformation employing a pentamethylated cyclopentadienyl (Cp*) iron complex and proposes a hypothesis as to why an alteration to the ligand design Significantly improved reaction efficiency and yield.

1.1 Previous Work

Previously, our group reported propargylic, allylic[20], and allenic[21, 22] C–H functionalization by employing a cationic pentasubstituted, cyclopentadienyl iron dicarbonyl complex (Cp^{R}Fe(CO)^2) (Figure 1A). Of particular interest is the catalytic, allenic functionalization as it represents the synthesis of new sp^2 C–C bonds from an unreactive C–H bond resulting exclusively in 1,1-disubstituted allene products. Previous attempts to functionalize monosubstituted allenes have been reported though the scope was limited to electron deficient species.[23, 24] Electronically neutral allene functionalization via transition metal catalyst have been reported however the scope is either limited to di- or tri- substituted allenes or, without a directing group, resulted in the 1,3 substituted product with high regioselectivity.[25]

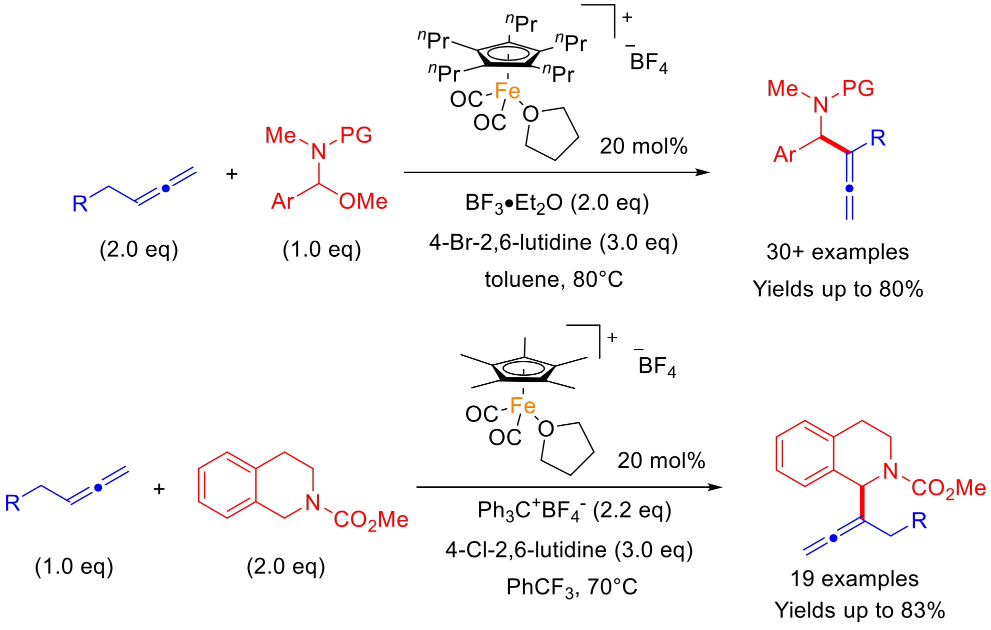

Figure 1: Synthesis of 1,1-disubstituted allenes using iron half-sandwich catalysts

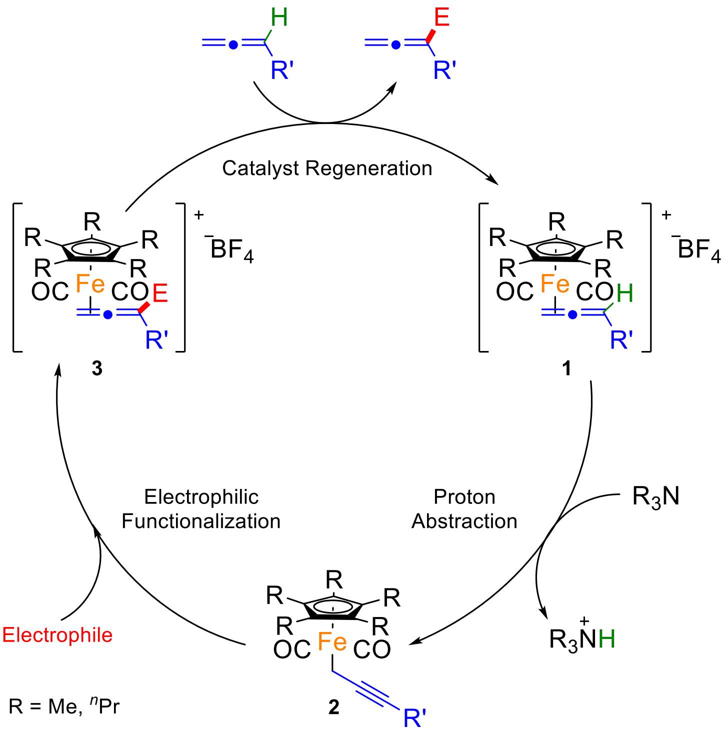

Figure 2: Proposed catalytic cycle for allenic C–H functionalization

The catalytic system we have developed provides mild conditions for the selective synthesis of 1,1-disubstituted allenes from monosubstituted derivatives. Such products can be achieved through the proposed catalytic cycle (Figure 1B). The precatalyst undergoes dissociation of a placeholder tetrahydrofuran (THF) ligand to allow uptake of monosubstituted allene and formation of an η^2-iron complex (**1**) with the π-bonds of the substrate. The proposed complexation would enhance the acidity of the α-C–H bonds such that proton abstraction could occur in the presence of weak pyridine bases. The resultant neutral, η^1-iron complexes (**2**) could then react with *in-situ* generated iminium electrophiles in an S_E2' fashion, generating a η^2-iron-1,1disubstituted allene complex (**3**). Regeneration of the catalytic iron core occurs through dissociation of the 1,1-disubstituted allene, followed by uptake of fresh substrate.

2.0 Results

Previous investigations began with synthesis of the proposed η^2-iron complex with the monosubstituted allene. These species were prepared in moderate yield using our groups precedented procedures with slight modifications from readily prepared iron iodide complexes discussed in Appendix A. The results afforded yellow to red-orange iron allene complexes which displayed atmospheric tolerance for up to 24 hours. ^{1}H-NMR spectroscopy analysis revealed the allenyl signals assuming an upfield shift of over 2.40 ppm. Such a dramatic difference alongside crystallographic data confirmed site exclusive binding by the metal center.

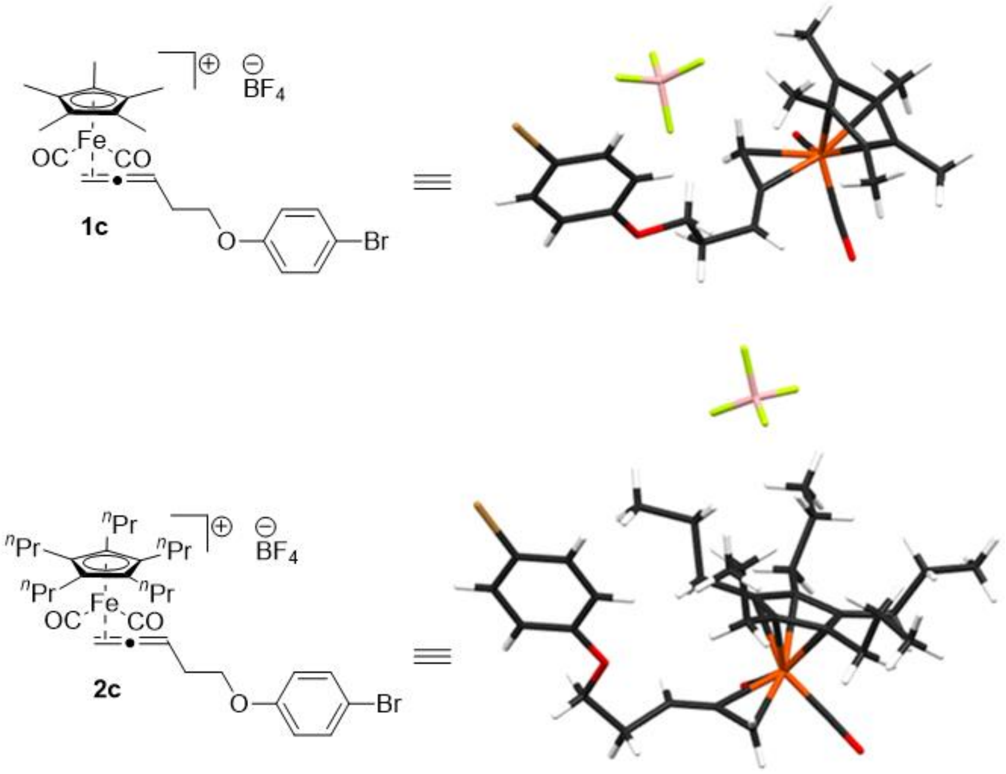

Figure 3: Crystal structures of compounds 1c ([$C_{23}H_{26}O_3BrFe$]$^{+[}$BF$_4$]$^-$, top) and 2c ([$C_{33}H_{46}O_3BrFe$]$^+$[BF$_4$]$^-$, bottom).

The allene assumes a bent geometry with a highly distorted C–C–C bond angle between 152.6-149.6° as well as a slightly distorted C–C–H bond angle of 118.1-116.9°. The Cp_{center} to metal bond length of 1.74 Å is consistent with other low spin cyclopentadienyl iron species.[26, 27]

2.1 Preliminary Mechanistic Experiments

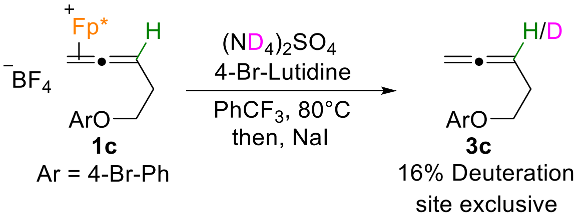

Figure 4: Deuterium exchange experiment

Earlier investigations included a deuterium exchange experiment to determine the site of the proposed deprotonation step.[21] The iron allene complex (**1c**) was exposed to 4-bromolutidine in the presence of D^+ ($(ND_4)_2SO_4$). Analysis of the decomplexated allene showed exclusive deuterium exchange at the allenic position (16%) (Figure 3). Attempts to isolate the propargyl iron (**2**) proved unsuccessful as direct exposure to base led to the formation of a complicated mixture of iron containing species. Additionally, we attempted to discern the rate determining step of the catalytic cycle. A primary kinetic isotope effect was studied using allene **f** and its isotopologue, selectively deuterated at the indicated allenic sp^2-C position (Figure 4).[22] Observations of the initial rates of the parallel reactions yielded a k_H/k_D of 3.3. This KIE result supports the proposition of a proton extraction at the indicated position when following the cycle from intermediates **1** to **3**.

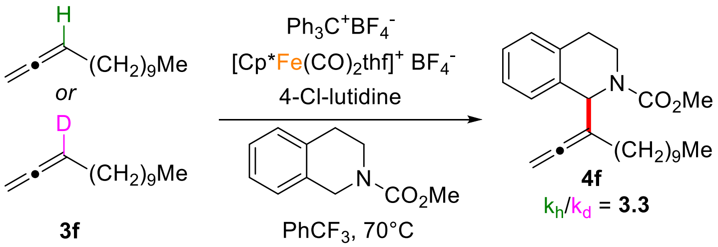

Figure 5: Primary KIE experiment

2.2 Further Mechanistic Experiments

In order to further support the proposed mechanism and in lieu of isolating the propargylic iron intermediate, a complimentary KIE experiment was performed using allene **3c** and its terminally D-H exchanged isotopologue **3c-*d*** (Figure 5). These parallel reactions provided yields which correspond to strong inverse secondary kinetic isotope effect with a k_H/k_D of 0.63. These results support our claims as the transformation from the η^2 to the η^1 iron complex (**1** to **2**) would necessitate a sp^2 to sp^3 shift for the terminal carbon atom of the allene.

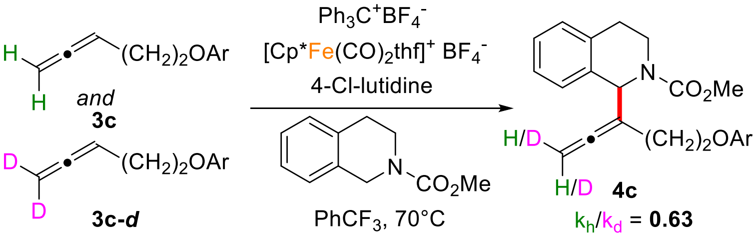

Figure 6: Secondary KIE experiment

The catalyst regeneration step had been previously explored using a monosubstituted allene and its difunctionalized counterpart.[22] This substrate exchange experiment provided preliminary results which displayed complete allene exchange at 48ºC after 3 hours. Due to the instability of the aforementioned iron-disubstituted allene complex, and in order to observe the initial rate kinetics of the catalyst regeneration, a model system was implemented using two commercially available allenes: 3-methyl-1,2-butadiene and cyclohexylallene. The exchange was measured by ^{1}H-NMR spectroscopy at 60ºC in $CDCl_3$ as lower temperatures afforded drastically slower exchange rates for the chosen substrates. The initial rate of exchange for both the Cp*Fe$(CO)_2$ and Cp$^{n\text{-}Pr}$Fe$(CO)_2$ complexes were recorded at various concentrations of allene and iron complex (Figure 6). The kinetic data is consistent with a first order rate with respect to the concentration of the iron complex.

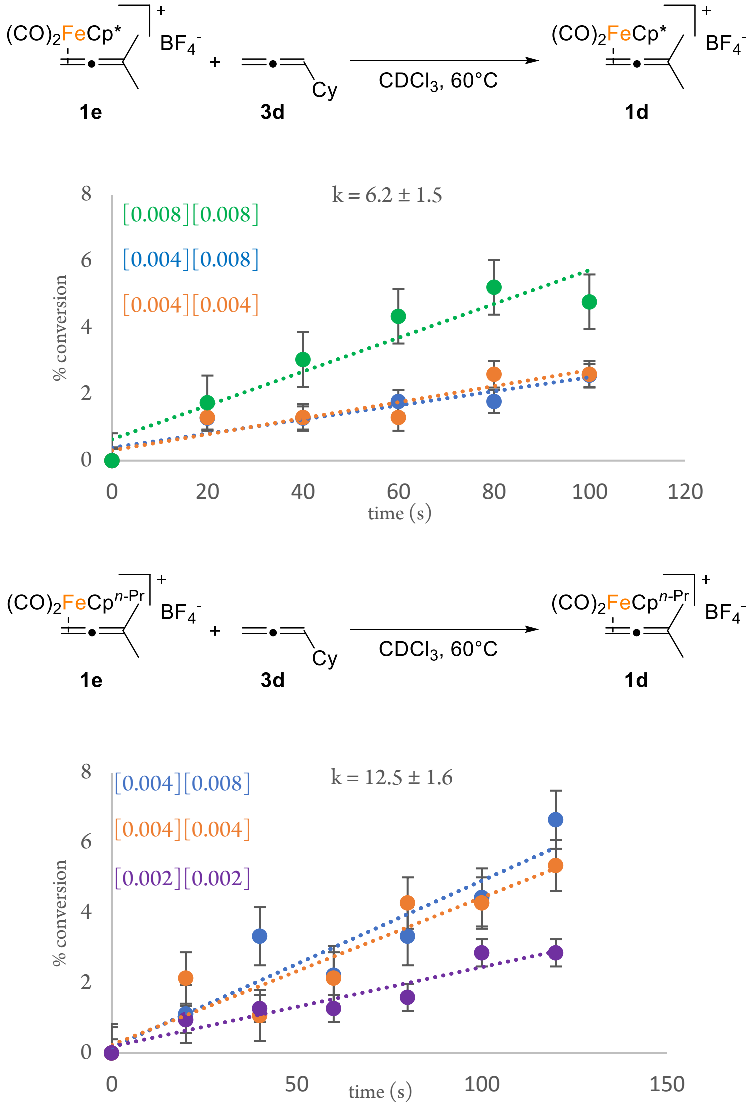

Figure 7: Initial exchange rates for Cp*Fe$(CO)_2$ 1e complex (top) and for Cp$^{n\text{-}Pr}$Fe$(CO)_2$ 2e complex (bottom). Concentrations are represented as [M][Allene]. Rates calculated for [0.004][0.004]

3.0 Discussion of Ligand Differences

Of note is the markedly faster exchange rate of the $Cp^{n\text{-}Pr}Fe(CO)_2$ (hereby denoted as Fp***) allene complex (**2e**) compared to the Fp* iron allene complexes. Investigations into the differences of these cousin ligands were encouraged by observations of minor to drastically improved yields for multiple systems previously explored by the group.[21, 22, 28] IR data of Fp*** and Fp* compounds with otherwise identical ligands revealed a shift in the carbonyl stretches averaging around 5 cm^{-1} more downfield for the pentapropylated complex. These differences suggest less backbonding into the π* orbital of the carbonyl ligand for Fp*** compoundsand is consistent with other metal systems known to be more electron deficient.[29, 30] Crystallographic data provides some insight as well (Table 1). The Cp_{center}–Fe distance for Fp*** is marginally shorter, consistent with low-spin, electron deficient systems. Additionally, the allene C–C–C bond angle deviates between the selected structures with the Fp*** having a less severely bent (152.6º) conformation compared to the Fp* (149.6º) as well as the C–C–H bond angle distorting in a similar way (Fp*** 116.9º) (Fp* 118.1º). The distance between the terminal carbon and the iron center was found to elongate as well when comparing the Fp* (2.134Å) to the Fp*** (2.149Å). We hypothesize that the orbital overlap of the *n*-propyl groups, according to the configuration they maintain in the crystal structure, is less intense than that of methyl groups leading to less electron density in the ring. This Fp*** system thus binds to the allene with adequate strength such that monosubstituted allenes do not readily displace, but disubstituted allenes do.

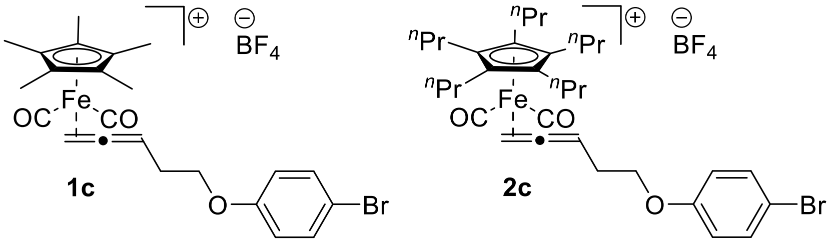

Figure 8: Selected iron half-sandwich structures

Table 1: Selected bond angles (º) and distances (Å) of the experimental structures of 1c and 2c

	1c	**2c**
C–C–C$_{\mathrm{allene}}$	149.6	152.6
C–C–H$_{\mathrm{allene}}$	118.1	116.9
Fe–Cp$_{\mathrm{center}}$	1.74	1.73
Fe–C	2.13	2.15

4.0 Conclusion

The mechanism for this iron-catalyzed, functionalization of allenic C(sp^2)–H bonds has been thoroughly analyzed. The transformation occurs through a proton abstraction exclusively at the allenic position leading to the organoiron species shifting from a cationic, π-bound allene configuration to a neutral, η^1-propargylic complex. This can then act as a nucleophile for *in-situ* generated electrophiles, performing a S_E2' reaction followed by a dissociative catalyst regeneration. We have also discussed how the subtle differences in ligand choice led to improved conditions by way of slight alterations to the electronics of the system. This communication should prove valuable to any future applications of this chemistry.

5.0 Experimental

5.1 General Information

General reagent information: Anhydrous toluene, dichloromethane, hexanes, tetrahydrofuran, and α,α,α-trifluorotoluene were purchased from Acros (AcroSeal packaging), Sigma Aldrich (Sure/Seal packaging), and Frontier Scientific (J&KSeal packaging), respectively, and were transferred into an argon-filled glovebox and used as received. Other dry solvents were obtained by distillation and storage over 3Å or 4Å molecular sieves. Triphenylcarbenium tetrafluoroborate ($Ph_3C^+BF^-$) was purchased from Sigma Aldrich and stored in an argon-filled glove box. All other reagents were purchased from Oakwood, Acros, Alfa Aesar, or Sigma Aldrich and used as received. Compounds were purified by flash column chromatography using SiliCycle SiliaFlash® F60 silica gel, unless otherwise indicated.

General analytical information: New compounds were characterized by ^{1}H NMR, ^{13}C NMR, HRMS and, where appropriate, other analytical techniques as indicated. Copies of the ^{1}H NMR and ^{13}C NMR spectra can be found at the end of the Supporting Information. ^{1}H, ^{2}H, ^{13}C, and ^{19}F NMR spectra were recorded on Bruker400 MHz or 500 MHz instruments. All ^{1}H NMR data are reported in δ units, parts per million (ppm), and were measured relative to the residual proton signal in the deuterated solvent at 7.26 ppm ($CDCl_3$) or 5.32 ppm (CD_2Cl_2). All ^{13}C NMR spectra are ^{1}H decoupled and reported in ppm relative to the solvent signal at 77.16 ppm ($CDCl_3$) or 53.84 ppm (CD_2Cl_2). Thin-layer chromatography (TLC) was performed on Silicycle 250 μm (analytical) or 1000 μm (preparative) silica gel plates. Compounds were visualized by irradiation with UV light, or by staining with potassium permanganate or cerium molybdate stain (Hanessian's stain). Yields refer to isolated compounds, unless otherwise indicated. High resolution mass spectra were recorded on a Thermo Scientific Q-Exactive mass spectrometer. NMR yield was determined by using 2,4-dinitrotolueneas internal standard for ^{1}H spectroscopy and using CD_2Cl_2 as the reference for ^{2}H spectroscopy. IR spectra were recorded on a PerkinElmer Spectrum Two FT-IR Spectrometer and are reported in terms of frequency of absorption (cm^{-1}).

5.2 Synthesis of organometallic compounds

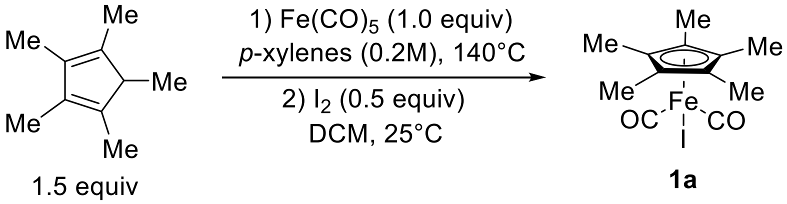

Figure 9: Synthesis of 1a

To a 100ml round bottom flask equipped with a Teflon coated magnetic stir bar, iron pentacarbonyl (0) (2.69 ml, 20 mmol, 2.0 equiv) and 1,2,3,4,5 pentamethylcyclopentadiene (1.56 ml, 10 mmol, 1.0 equiv) were dissolved in *p*-xylenes (20 ml) and set to stir at 140ºC for 24 hours. The reaction was allowed to cool to room temperature and the solvent was removed *in vacuo*. The reaction mixture was then dissolved in DCM and filtered over celite to remove insoluble material. The filter cake was washed until the solvent ran clear and the resultant filtrate was concentrated down until about 20 ml of it remained. Iodine (1.27 g, 5 mmol, 0.5 equiv) was added to the solution at room temperature and allowed to stir in the dark for 3 hours. The reaction mixture was quenched with aqueous sodium sulfite solution and extracted twice with DCM. The extract was washed with brine and dried over $MgSO_4$. The product was recrystallized from a black oil to afford a shiny black solid **1a** (2.412 g, 65% yield).

^{1}HNMR (400 MHz, CD_2Cl_2) δ 1.98

FTIR (cm^{-1}) 2001.99 (CO), 1948.50 (CO)

HRMS (ESI) calcd for $C_{22}H_{35}FeIO_2$ $[M+H]^+$: 373.94607, found 373.94477

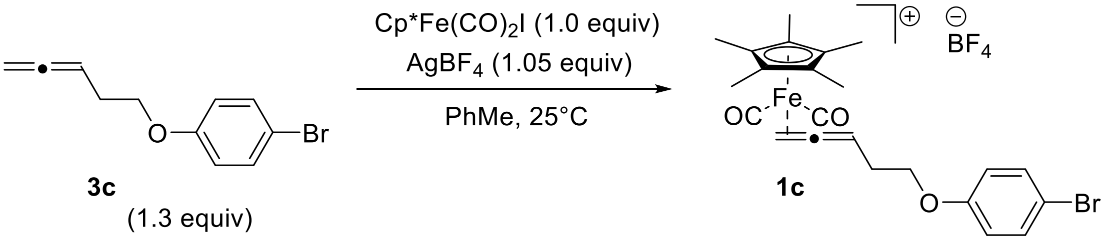

Figure 10: Synthesis of 1c

Under an argon atmosphere, 1-bromo-4-(penta-3,4-dien-1-yloxy)benzene **3c** (179 mg, 0.75 mmol, 1.5 equiv) was added to a reaction tube (13 mm × 100 mm, Fisherbrand, part # 14-959-35C) charged with $Cp^*Fe(CO)_2I$ (188 mg, 0.5mmol, 1.0 equiv), $AgBF_4$ (97 mg, 0.51 mmol, 1.05 equiv) and a Teflon-coated magnetic stir bar. The mixture was then suspended in 0.1ml of dry toluene and set to stir at room temperature, in the dark, for 6 hours. The reaction mixture was then diluted with n-hexanes and filtered over Celite. The filter cake was generously washed with excess n-hexanes. The filter cake was then rinsed with dry dichloromethane until the filtrate ran colorless. The filtrate was then concentrated in vacuo resulting in an orange solid. (249 mg, 85% yield)

^{1}HNMR (400 MHz, $CDCl_3$) δ 7.40 (d, 2H), 6.78 (d, 2H), 6.04 (br, 1H), 4.18 (br, 2H), 2.95 (br, 2H), 2.60 (br, 2H), 1.91 (s, 15H)

FTIR (cm^{-1}) 2051.50 (CO), 2026.67 (CO)

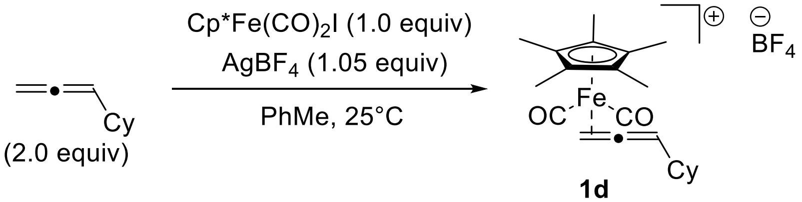

Figure 11: Synthesis of 1d

Under an argon atmosphere, cyclohexylallene (156µl, 1.08mmol, 2.0 equiv) was added to a reaction tube (13 mm × 100 mm, Fisherbrand, part # 14-959-35C) charged with Cp*Fe(CO)$_2$I (200 mg, 0.54 mmol, 1.0 equiv), AgBF$_4$ (110 mg, 0.57 mmol, 1.05 equiv) and a Teflon-coated magnetic stir bar. The mixture was then suspended in 0.5ml of dry toluene and set to stir at room temperature, in the dark, for 4 hours. The reaction mixture was then diluted with n-hexanes and filtered over Celite. The filter cake was generously washed with excess n-hexanes. The filter cake was then rinsed with dry dichloromethane until the filtrate ran colorless. The filtrate was then concentrated in vacuo resulting in a tan-yellow solid **1d**. (163 mg, 82% yield)

^{1}HNMR (400 MHz, CD$_2$Cl$_2$) δ 5.90 (s, 1H), 2.55 (s, 2H), 2.38 (br, 1H), 1.88 (s, 15H), 1.79 (m, 2H), 1.70 (m, 2H), 1.28 (m, 6H)

^{19}FNMR (376MHz, CD$_2$Cl$_2$) δ -152.6

^{13}CNMR (125MHz, CD$_2$Cl$_2$) δ 210.98, 155.62, 124.85, 103.60, 43.51, 32.70, 25.96, 25.91, 22.51, 9.20

FTIR (cm^{-1}) 2049.19 (CO), 2014.03 (CO)

HRMS (ESI) calcd for $C_{21}H_{29}FeO_2$ [M-BF$_4^-$]$^+$: 369.15115, found 369.15094

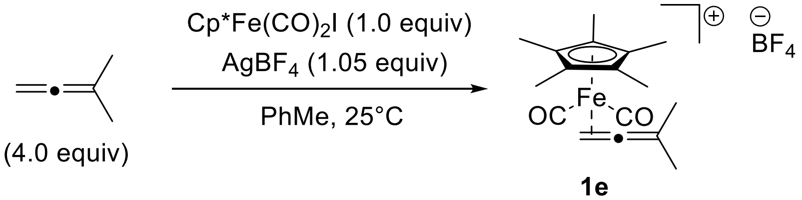

1e

Figure 12: Synthesis of 1e

Under an argon atmosphere, 3-methyl-1,2 butadiene (210 µl, 2.16 mmol, 4.0 equiv) was added to a reaction tube (13 mm × 100 mm, Fisherbrand, part # 14-959-35C) charged with Cp*Fe(CO)$_2$I (200 mg, 0.54 mmol, 1.0 equiv), AgBF$_4$ (110 mg, 0.57 mmol, 1.05 equiv) and a

Teflon-coated magnetic stir bar. The mixture was then suspended in 0.5ml of dry toluene and set to stir at room temperature, in the dark, for 4 hours. The reaction mixture was then diluted with n-hexanes and filtered over Celite. The filter cake was generously washed with excess n-hexanes. The filter cake was then rinsed with dry dichloromethane until the filtrate ran colorless. The filtrate was then concentrated in vacuo resulting in a red-orange solid **1e**. (165 mg, 76% yield)

^{1}HNMR (400 MHz, CD_2Cl_2) δ 2.36 (s, 2H), 2.24 (br, 3H), 2.12 (br, 3H), 1.91 (s, 15H)

^{19}FNMR (376MHz, CD_2Cl_2) δ -150.93, -150.98

^{13}CNMR (125MHz, CD_2Cl_2) δ 210.67, 151.16, 122.56, 104.17, 97.74, 30.53, 23.36, 9.51

FTIR (cm^{-1}) 2058.33 (CO), 2016.90 (CO)

HRMS (ESI) calcd for $C_{17}H_{23}FeO_2$ [M-BF_4^-]$^+$: 315.10420, found: 315.10345

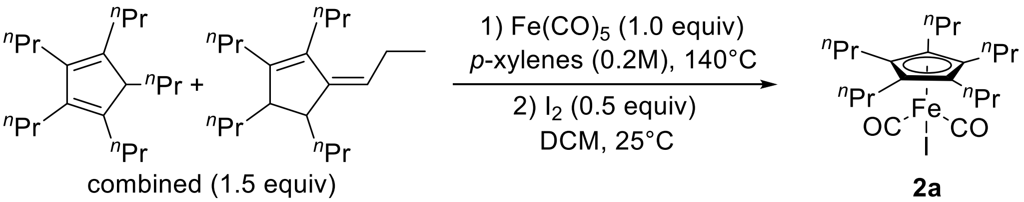

Figure 13: Synthesis of 2a

To a 100ml round bottom flask equipped with a Teflon coated magnetic stir bar, iron pentacarbonyl (0) (0.55 ml, 4 mmol, 1.0 equiv) and 1,2,3,4,5 pentapropylcyclopentadiene (1.66 g, 6 mmol, 1.5 equiv) were dissolved in *p*-xylenes (20 ml) and set to stir at 140ºC for 24 hours. The reaction was allowed to cool to room temperature and the solvent was removed *in vacuo*. The reaction mixture was then dissolved in DCM and filtered over celite to remove insoluble material. The filter cake was washed until the solvent ran clear and the resultant filtrate was concentrated down until about 20 ml of it remained. Iodine (508 mg, 2 mmol, 0.5 equiv) was added to the solution at room temperature and allowed to stir in the dark for 3 hours. The reaction mixture was quenched with aqueous sodium sulfite solution and extracted twice with DCM. The extract was washed with brine and dried over $MgSO_4$. Column chromatography (SiO_2, hexanes/ethyl acetate, 40:1) afforded the shiny black solid **2a** (861 mg, 42% yield).

^{1}HNMR (400 MHz, CD_2Cl_2) δ 2.26 (m, 10H), 1.49 (m, 10H), 1.01 (t, 15H).

FTIR (cm^{-1}) 2012.20 (CO), 1965.19 (CO)

HRMS (ESI) calcd for $C_{22}H_{35}FeIO_2$ $[M+H]^+$: 514.10257, found 514.10278

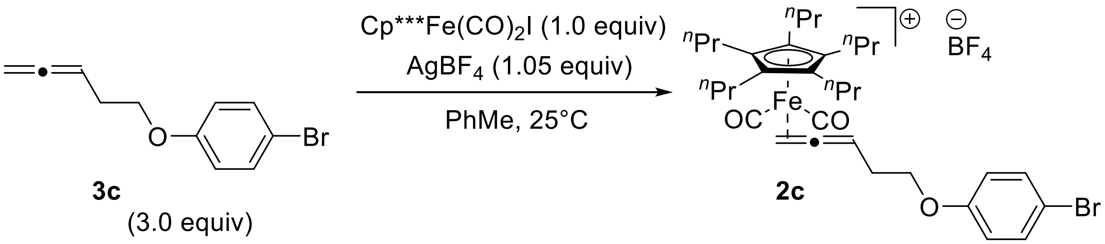

Figure 14: Synthesis of 2c

Under an argon atmosphere, 1-bromo-4-(penta-3,4-dien-1-yloxy)benzene **3c** (62 mg, 0.26 mmol, 1.3 equiv) was added to a reaction tube (13 mm × 100 mm, Fisherbrand, part # 14-959-35C) charged with Cp***Fe(CO)$_2$I (102mg, 0.2mmol, 1.0 equiv), $AgBF_4$ (40 mg, 0.21 mmol, 1.05 equiv) and a Teflon-coated magnetic stir bar. The mixture was then suspended in 0.1ml of dry toluene and set to stir at room temperature, in the dark, for 2 hours. The reaction mixture was then diluted with n-hexanes and filtered over Celite. The filter cake was generously washed with excess n-hexanes. The filter cake was then rinsed with dry dichloromethane until the filtrate ran colorless. The filtrate was then concentrated in vacuo resulting in a tan-yellow solid. (78 mg, 54% yield)

^{1}HNMR (400 MHz, CD_2Cl_2) δ 7.39 (2H), 6.83 (2H), 6.09 (1H), 4.19 (2H), 2.93 (2H), 2.71 (2H), 2.20 (10H), 1.51 (10H), 1.06 (15H)

^{19}FNMR (376MHz, CD_2Cl_2) δ -150.19

^{13}CNMR (126 MHz, CD_2Cl_2) δ 210.19, 157.89, 157.59, 132.52, 117.03, 116.36, 107.22, 102.07, 66.91, 35.57, 26.95, 24.23, 23.02, 14.73

FTIR (cm^{-1}) 2064.33 (CO), 2010.03 (CO)

HRMS (ESI) calcd for $C_{34}H_{49}FeBrO_3$ $[M-BF_4^-]^+$: 625.19743, found 625.19726

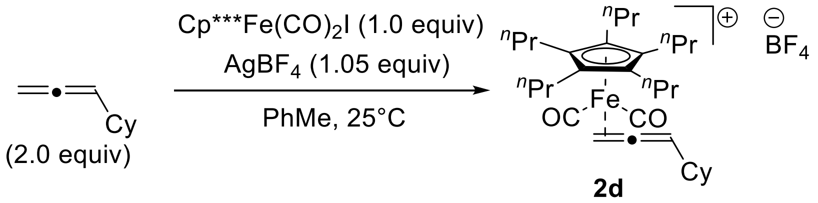

Figure 15: Synthesis of 2d

Under an argon atmosphere, cyclohexylallene (32 µl, 0.2 mmol, 2.0 equiv) was added to a reaction tube (13 mm × 100 mm, Fisherbrand, part # 14-959-35C) charged with Cp***Fe$(CO)_2$I (51mg, 0.1mmol, 1.0 equiv), $AgBF_4$ (110 mg, 0.57 mmol, 1.05 equiv) and a Teflon-coated magnetic stir bar. The mixture was then suspended in 0.1ml of dry toluene and set to stir at room temperature, in the dark, for 4 hours. The reaction mixture was then diluted with n-hexanes and filtered over Celite. The filter cake was generously washed with excess n-hexanes. The filter cake was then rinsed with dry dichloromethane until the filtrate ran colorless. The filtrate was then concentrated in vacuo resulting in a tan-yellow solid. (33 mg, 53% yield)

^{1}HNMR (400 MHz, CD_2Cl_2) δ 5.89 (dt, 1H), 2.64 (dd, 2H), 2.16 (m, 10H), 1.87 (m, 2H), 1.77 (m, 2H), 1.68 (m, 1H), 1.51 (m, 10H), 1.33 (m, 2H), 1.22 (m, 4H), 1.08 (t, 15H)

^{19}FNMR (376MHz, CD_2Cl_2) δ -152.20

^{13}CNMR (101MHz, CD_2Cl_2) δ 210.44, 154.98, 124.94, 106.73, 106.73, 43.51, 32.50, 26.96, 25.88, 24.17, 23.20, 14.72.

FTIR (cm^{-1}) 2053.51 (CO), 2018.56 (CO)

HRMS (ESI) calcd for $C_{31}H_{49}FeO_2$ $[M-BF_4^-]^+$: 509.30765, found 509.30601

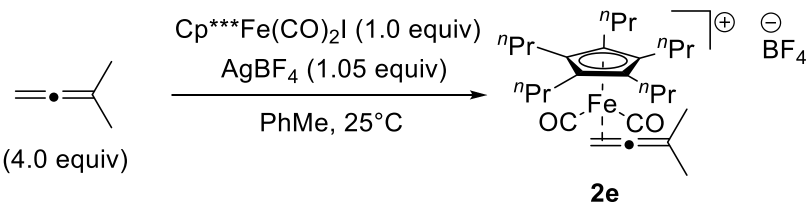

2e

Figure 16: Synthesis of 1e

Under an argon atmosphere, 3-methyl-1,2 butadiene (39µl, 0.4mmol, 4.0 equiv) was added to a reaction tube (13 mm × 100 mm, Fisherbrand, part # 14-959-35C) charged with Cp***Fe(CO)$_2$I (51mg, 0.1mmol, 1.0 equiv), AgBF$_4$ (23mg, 0.57mmol, 1.05 equiv) and a Teflon-coated magnetic stir bar. The mixture was then suspended in 0.1ml of dry toluene and set to stir at room temperature, in the dark, for 1 hour. The reaction mixture was then diluted with n-hexanes and filtered over Celite. The filter cake was generously washed with excess n-hexanes. The filter cake was then rinsed with dry dichloromethane until the filtrate ran colorless. The filtrate was then concentrated in vacuo. The solid was then washed with a 5ml solution of 5%DCM in toluene to remove leftover iron iodide. This resulted in a pale orange solid. (31 mg, 59% yield)

^{1}HNMR (400 MHz, CD$_2$Cl$_2$) δ 2.12 (s, 2H), 2.09 (m, 10H), 1.60 (s, 3H), 1.49 (m, 13H), 1.03 (t, 15H)

^{19}FNMR (376MHz, CD$_2$Cl$_2$) δ -148.73, -150.97

^{13}CNMR: Compound proved to be too unstable to measure by ^{13}CNMR

FTIR (cm^{-1}) 2062.80 (CO), 2027.64 (CO)

HRMS (ESI) calcd for $C_{27}H_{43}FeO_2$ [M-BF$_4^-$]$^+$: 455.26070, found 455.25995

5.3 Synthesis of organic compounds

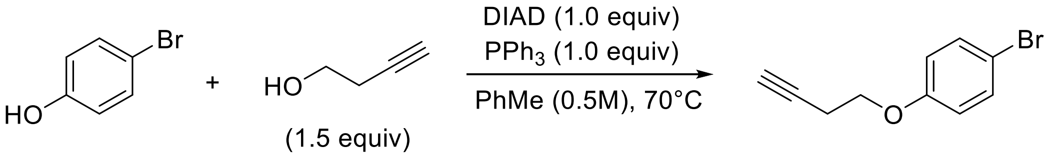

Figure 17: Synthesis of precursor to 3c

To a 250 ml round bottom flask equipped with a Teflon-coated magnetic stir bar, 4-bromophenol (3.460 g, 20 mmol, 1.0 equiv), triphenylphosphine (5.240 g, 20 mmol, 1.0 equiv), and 3-butyn-1-ol (1.51 ml, 22 mmol, 1.1 equiv) were dissolved in toluene (20 ml) and cooled to 0ºC. Diisopropyl azodicarboxylate (DIAD) (4.041 g, 20 mmol, 1.0 equiv) was added dropwise to the stirring solution. The reaction was then heated to 70ºC for 3.5 hours. The mixture was allowed to cool to room temperature before being diluted with hexanes (40 ml) and filtered through a pad of celite. This process was repeated two additional times. The solvent removed in vacuo and the crude product was purified via flash chromatography (SiO_2, hexanes/ethyl acetate 40:1) to yield the alkyne as a colorless oil (1.940 g, 43% yield).

^{1}HNMR (400 MHz, $CDCl_3$) δ 7.36 (m, 2H), 6.78 (m, 2H), 5.21 (t, 1H), 4.00 (t, 2H), 2.48 (q, 2H)

HRMS (ESI) calcd for $C_{10}H_9BrO$ $[M+H]^+$: 224.99095, found 224.99086

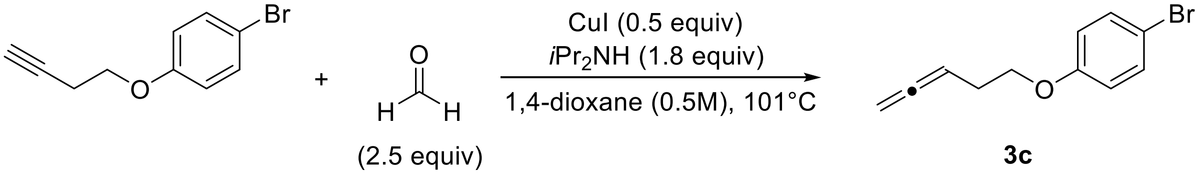

3c

Figure 18: Synthesis of 3c

To a 100 ml round bottom flask equipped with a Teflon-coated magnetic stir bar, copper iodide (336 mg, 1.75 mmol, 0.5 equiv) and paraformaldehyde (265 mg, 8.75 mmol, 2.5 equiv) were added and placed under a N_2 atmosphere. The solids were submerged in 1,4-dioxane (17.5 ml) and alkyne (790 mg, 3.5 mmol, 1.0 equiv) was added via syringe and the mixture was stirred. Diisopropylamine (0.88 ml, 6.3 mmol, 1.8 equiv) was added dropwise to the stirring solution. The mixture was then heated to 110ºC and stirred for 4 hours. The reaction was allowed to cool to room temperature before being quenched with water (20 ml) and then filtered through celite. The aqueous layer was extracted with ethyl acetate (2x20 ml) and the combined organic layers were washed with brine and dried over $MgSO_4$. Solvent was removed in vacuo and the crude product was purified via flash chromatography (SiO2, hexanes/ethyl acetate 50:1) to yield **3c** as a yellow oil (394 mg, 47% yield).

^{1}HNMR (400 MHz, $CDCl_3$) δ 7.36 (m, 2H), 6.78 (m, 2H), 5.20 (p, 1H), 4.73 (m, 2H), 4.00 (t, 2H), 2.48 (m, 2H)

HRMS (ESI) calcd for $C_{11}H_{11}BrO$ $[M+H]^+$: 239.0066, found 239.0071

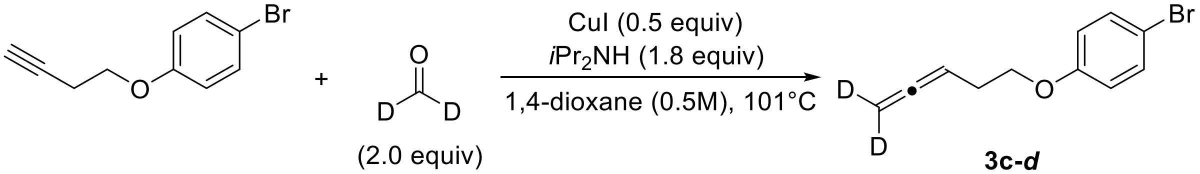

Figure 19: Synthesis of 3c-*d*

To a 100 ml round bottom flask equipped with a Teflon-coated magnetic stir bar, copper iodide (275 mg, 1.5 mmol, 0.5 equiv) and paraformaldehyde-d_2 (187 mg, 5.8 mmol, 2.0 equiv) were added and placed under a N_2 atmosphere. The solids were submerged in 1,4-dioxane (15 ml) and alkyne (655 mg, 2.9 mmol, 1.0 equiv) was added via syringe and the mixture was stirred. Diisopropylamine (0.728 ml, 5.2 mmol, 1.8 equiv) was added dropwise to the stirring solution. The mixture was then heated to 110ºC and stirred for 4 hours. The reaction was allowed to cool to room temperature before being quenched with water (20 ml) and then filtered through celite. The aqueous layer was extracted with ethyl acetate (2x20 ml) and the combined organic layers were washed with brine and dried over $MgSO_4$. Solvent was removed in vacuo and the crude product was purified via flash chromatography (SiO2, hexanes/ethyl acetate 50:1) to yield **3c-*d*** as a yellow oil (394 mg, 40% yield).

^{1}HNMR (400 MHz, $CDCl_3$) δ 7.36 (d, 2H), 6.78 (d, 2H), 5.21 (t, 1H), 4.00 (t, 2H), 2.48 (q, 2H)

^{2}HNMR (61.44 MHz, CH_2Cl_2) δ 4.71

^{13}CNMR (100MHz, CD_2Cl_2) δ 209.13, 158.24, 132.28 (s, 2C), 116.49 (s, 2C), 112.70, 86.30, 74.64 (p, 1C), 67.55, 28.32

HRMS (ESI) calcd for $C_{11}H_9D_2BrO$ $[M+H]^+$: 241.01916, found 241.01973

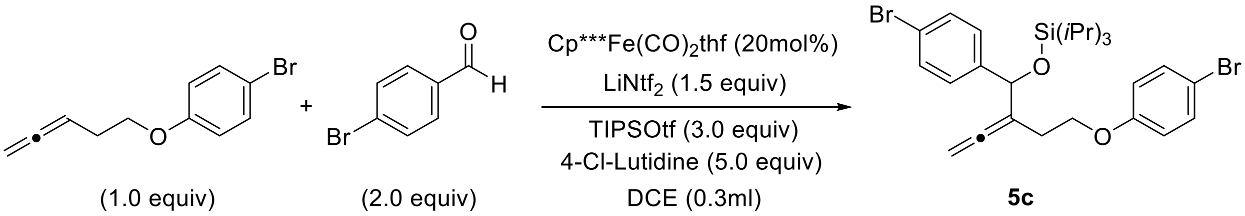

Figure 20: Synthesis of 5c

In an argon filled glovebox, aldehyde (73.2 mg, 0.4 mmol, 2.0 equiv) was combined with lithium bistriflimide (86.2 mg, 0.3 mmol, 1.5 equiv), iron catalyst (21.8 mg, 0.04 mmol, 0.2 equiv), triisopropylsilyl trifluoromethanesulfonate (160 µl, 0.6 mmol, 3.0 equiv), allene, (47.8 mg, 0.2 mmol, 1.0 equiv), and 4-Cl-lutidine (130 µl, 1.0 mmol, 5.0 equiv) in a reaction tube (13 mm × 100 mm, Fisherbrand, part # 14-959-35C) and submerged in dichloroethane (0.3 ml). The tube was capped and removed from the glovebox. The vessel was moved to an oil bath preheated to 80ºC. After 1 hour had eclipsed the reaction was taken off of heat and purified via flash chromatography (SiO2, hexanes/ethyl acetate, 20:1), resulting in a colorless oil **5c** (90.2 mg, 78% yield).

^{1}HNMR (400 MHz, $CDCl_3$) δ 7.40 (m, 2H), 7.24 (m, 4H), 6.60 (m, 2H), 5.39 (s, 1H), 4.82 (m, 2H), 3.82 (dtd, 2H), 2.40 (dddd, 1H), 2.06 (dddd, 1H), 1.09 (m, 3H), 1.00 (d, 18H)

HRMS (ESI) calcd for $C_{27}H_{36}Br_2SiO_2$ $[M+H]^+$: 579.09241, found 579.09184

5.4 Kinetic exchange experiments

5.4.1 Complete Exchange

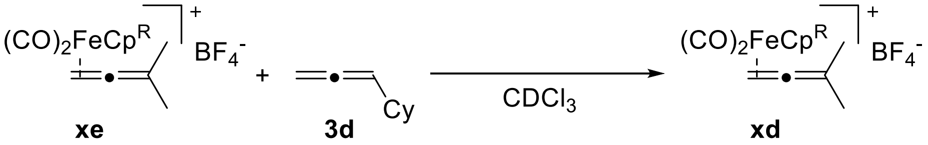

Figure 21: Model system for ligand exchange

In an argon-filled glovebox, 1e (8.0 mg, 20 µmol, 1.0 equiv) was added to an NMR tube and dissolved in CDCl3 (0.5 mL). Then allene 3d (2.89 µl, 20 µmol, 1.0 equiv) was added to the above solution. The NMR tube was capped and sealed with parafilm. Then the NMR tube was placed under dark, and the reaction was monitored by 1H NMR using 2,4-dinitrotoluene as internal standard at 75ºC. The exchange was complete after 1.5 hours.

In an argon-filled glovebox, 2e (11 mg, 20 µmol, 1.0 equiv) was added to an NMR tube and dissolved in CDCl3 (0.5 mL). Then allene 3d (2.86 µl, 20 µmol, 1.0 equiv) was added to the above solution. The NMR tube was capped and sealed with parafilm. Then the NMR tube was placed under dark, and the reaction was monitored by 1H NMR using 2,4-dinitrotoluene as internal standard at 75ºC. The exchange was complete after 1 hour.

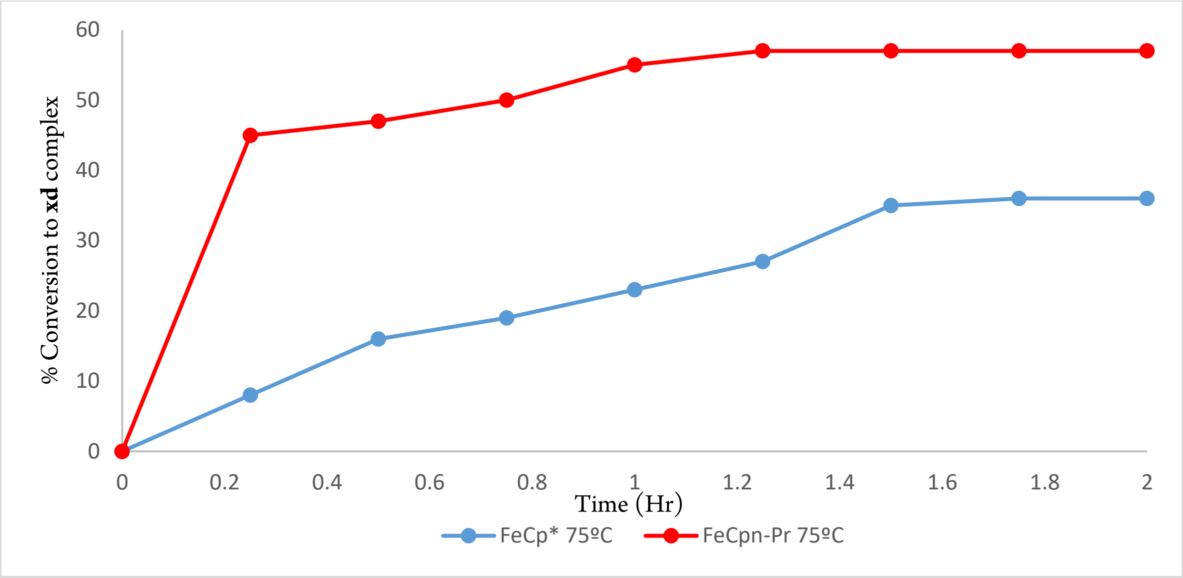

Figure 22: Complete exchange of model system

5.4.2 Initial Kinetics

In an argon-filled glovebox, 1e (8 mg, 20 µmol, 1.0 equiv) was added to an NMR tube and dissolved in CDCl3 (0.5 mL). Then, allene 3d (2.86 µl, 20 µmol, 1.0 equiv) was added to the above solution. The NMR tube was capped and sealed with parafilm. Then the NMR tube was placed under dark, and the reaction was monitored by 1H NMR using 2,4-dinitrotoluene as internal standard at 60ºC. Spectra were collected once every 20 seconds for one hour.

In an argon-filled glovebox, 2e (11 mg, 20 µmol, 1.0 equiv) was added to an NMR tube and dissolved in CDCl3 (0.5 mL). Then, allene 3d (2.86 µl, 20 µmol, 1.0 equiv) was added to the above solution. The NMR tube was capped and sealed with parafilm. Then the NMR tube was placed under dark, and the reaction was monitored by 1H NMR using 2,4-dinitrotoluene as internal standard at 60ºC. Spectra were collected once every 20 seconds for one hour.

5.5 Secondary inverse KIE experiment

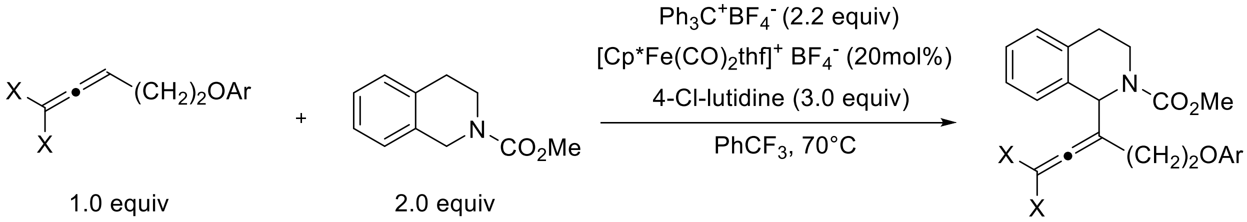

Figure 23: Synthesis of 4c

In an argon filled glovebox, tetrahydroisoquinoline (38.2 ml, 0.2 mmol, 2.0 equiv) was combined with tritylium tetrafluoroborate (72.6 mg, 0.22 mmol, 2.2 equiv) in a reaction tube (13 mm × 100 mm, Fisherbrand, part # 14-959-35C) and submerged in trifluorotoluene (0.2 ml). The tube was capped and set to stir under an argon atmosphere. After 3 hours of stirring, allene (**3c**) (0.1 mmol, 1.0 equiv) was introduced followed by iron catalyst (8.1 mg, 0.02 mmol, 0.2 equiv) and finally 4-Cl-lutidine (38.2 µl, 0.3 mmol, 3.0 equiv). The reaction vessel was capped and moved to an oil bath preheated to 70ºC. After 1 hour had eclipsed the reaction was taken off of heat and purified via flash chromatography (SiO_2, hexanes/acetone, 9:1).

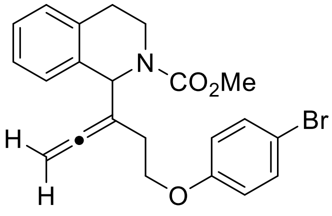

4c

^{1}HNMR (400 MHz, $CDCl_3$) δ 7.37 (m, 2H), 7.16 (m, 4H), 6.79 (m, 2H), 5.74 (br, 1H), 4.65 (m, 2H), 4.08 (t, 1H), 3.77 (d, 3H), 3.42 (br, 1H), 2.89 (br, 1H), 2.80 (dt, 1H), 2.53 (br, 1H)

HRMS (ESI) calcd for $C_{22}H_{22}BrNO_3$ $[M+H]^+$: 428.08558, found 428.08559

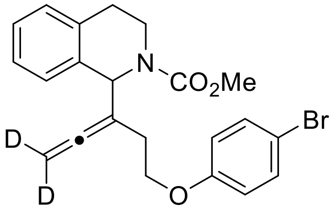

4c-*d*

^{1}HNMR (400 MHz, $CDCl_3$) δ 7.36 (m, 2H), 7.13 (m, 4H), 6.77 (m, 2H), 5.72 (br, 1H), 4.05 (t, 2.5H), 3.37 (s, 3.5H), 3.40 (br, 1H), 2.91 (br, 1H), 2.79 (dt, 1H), 2.50 (br, 1H)

^{2}HNMR (61.44 MHz, CH_2Cl_2) δ 4.58

HRMS (ESI) calcd for $C_{22}H_{20}D_2BrNO_3$ $[M+H]^+$: 430.09868, found 430.09784

Appendix A : NMR Spectra

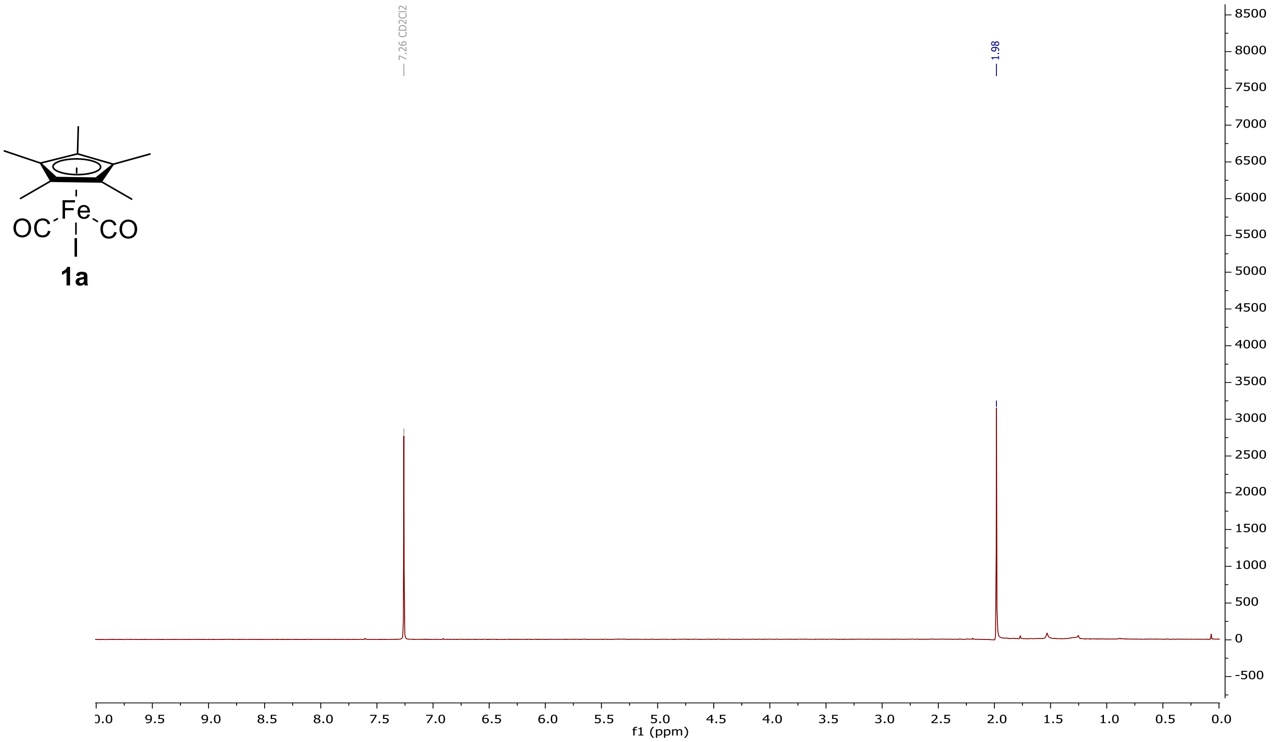

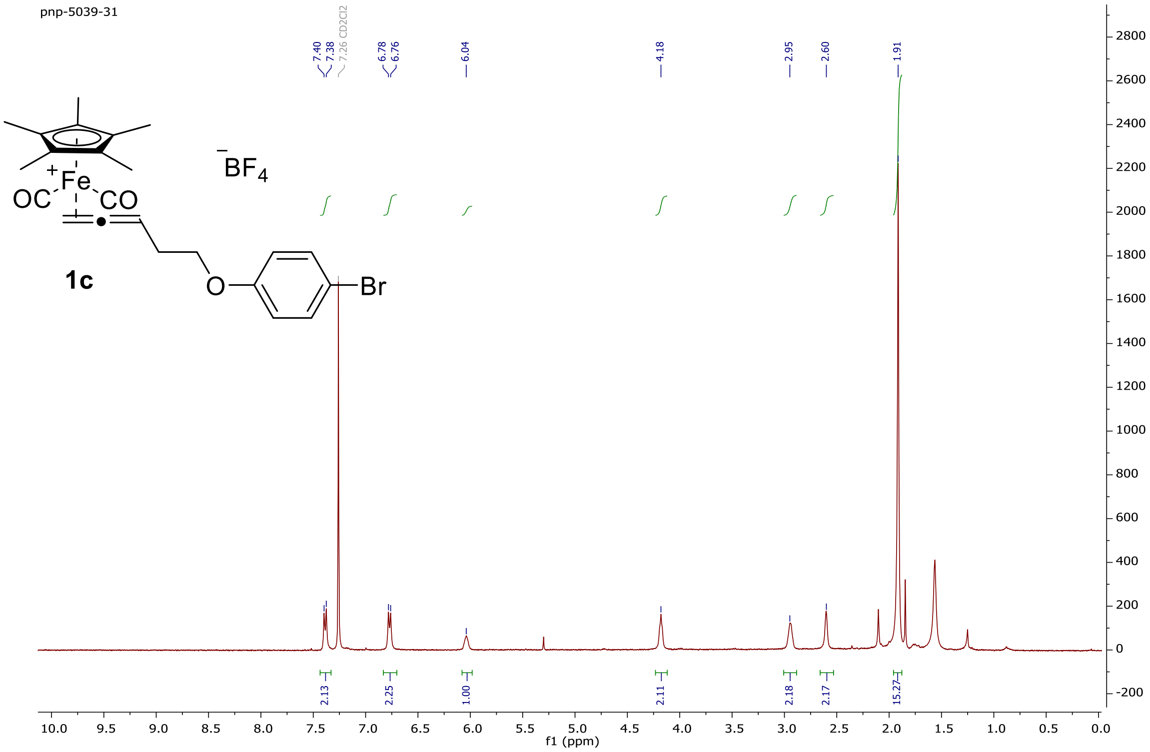

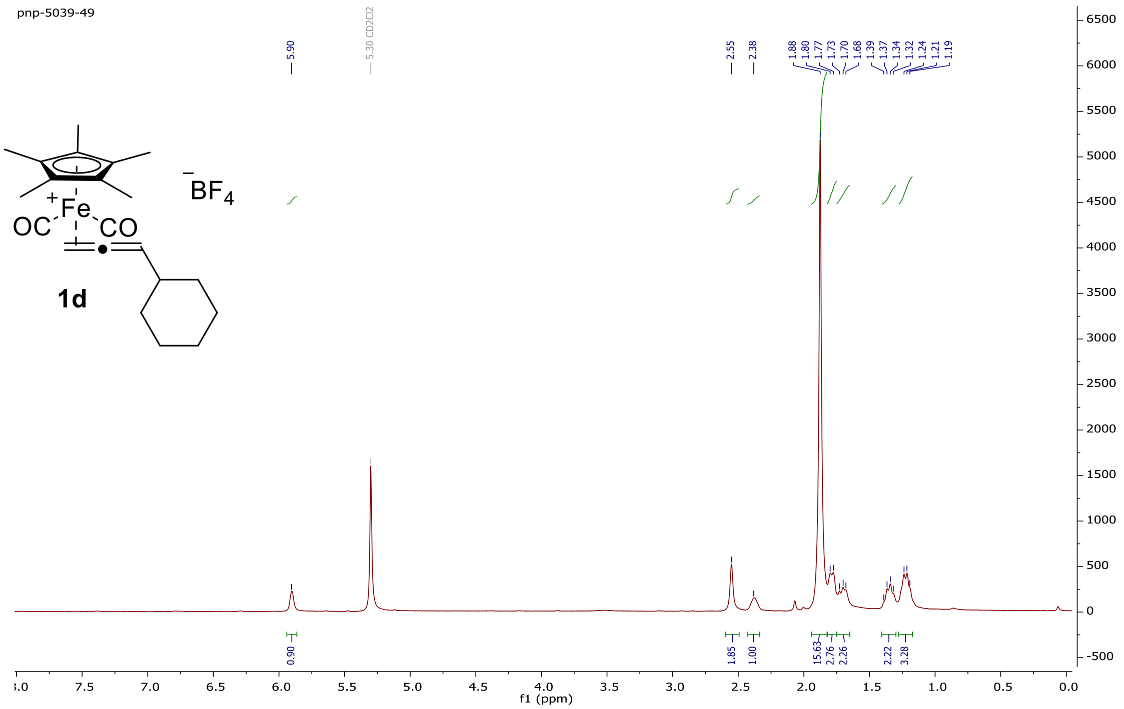
pnp-5039-49
5.90
5.30 CD2Cl2
2.55
2.38
1.88
1.80
1.77
1.73
1.70
1.68
1.39
1.37
1.34
1.32
1.24
1.21
1.19
0.90
1.85
1.00
15.63
2.76
2.26
2.22
3.28
+Fe
OC
CO
BF4
1d
f1 (ppm)

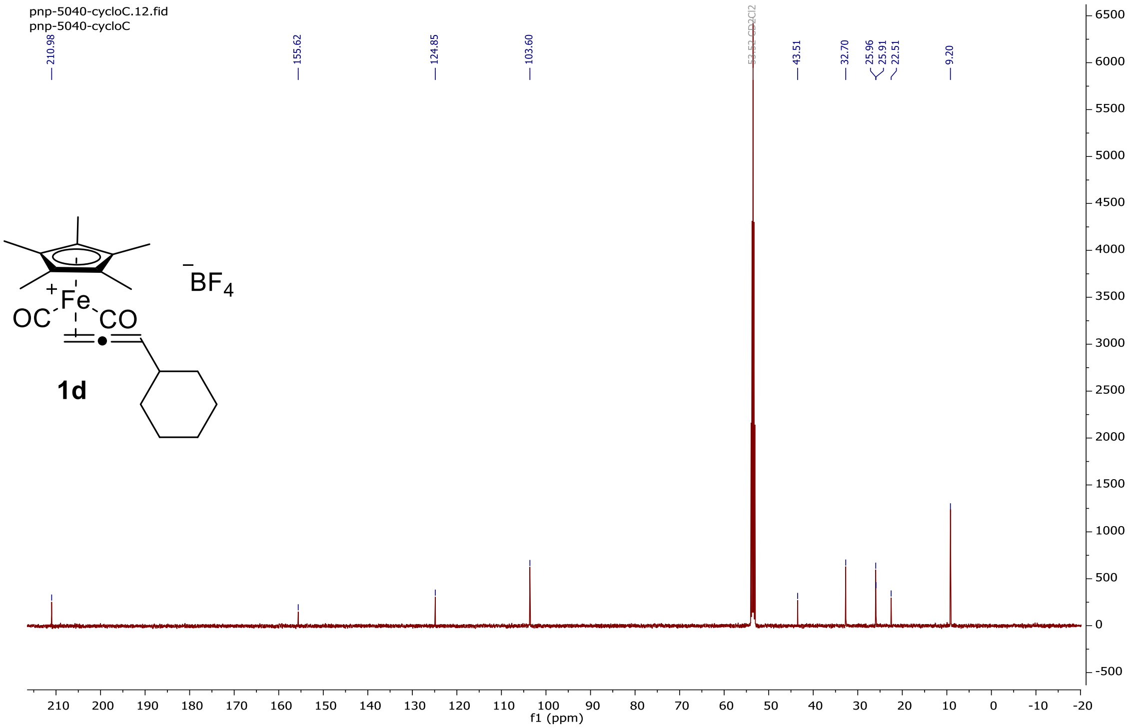
pnp-5040-cycloC.12.fid
pnp-5040-cycloC
210.98
155.62
124.85
103.60
53.52 CD2Cl2
43.51
32.70
25.96
25.91
22.51
9.20
+Fe
OC
CO
BF4
1d
f1 (ppm)

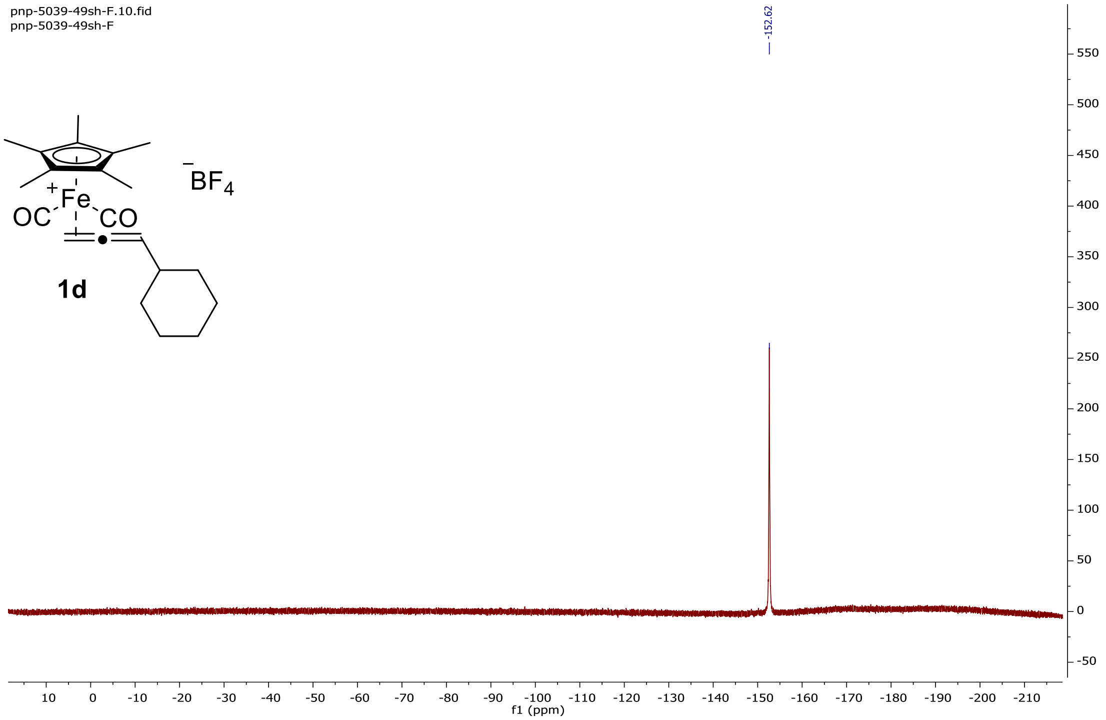
pnp-5039-49sh-F.10.fid
pnp-5039-49sh-F
-152.62
1d
BF4
Fe
OC
CO
f1 (ppm)
10 0 -10 -20 -30 -40 -50 -60 -70 -80 -90 -100 -110 -120 -130 -140 -150 -160 -170 -180 -190 -200 -210
550 500 450 400 350 300 250 200 150 100 50 0 -50

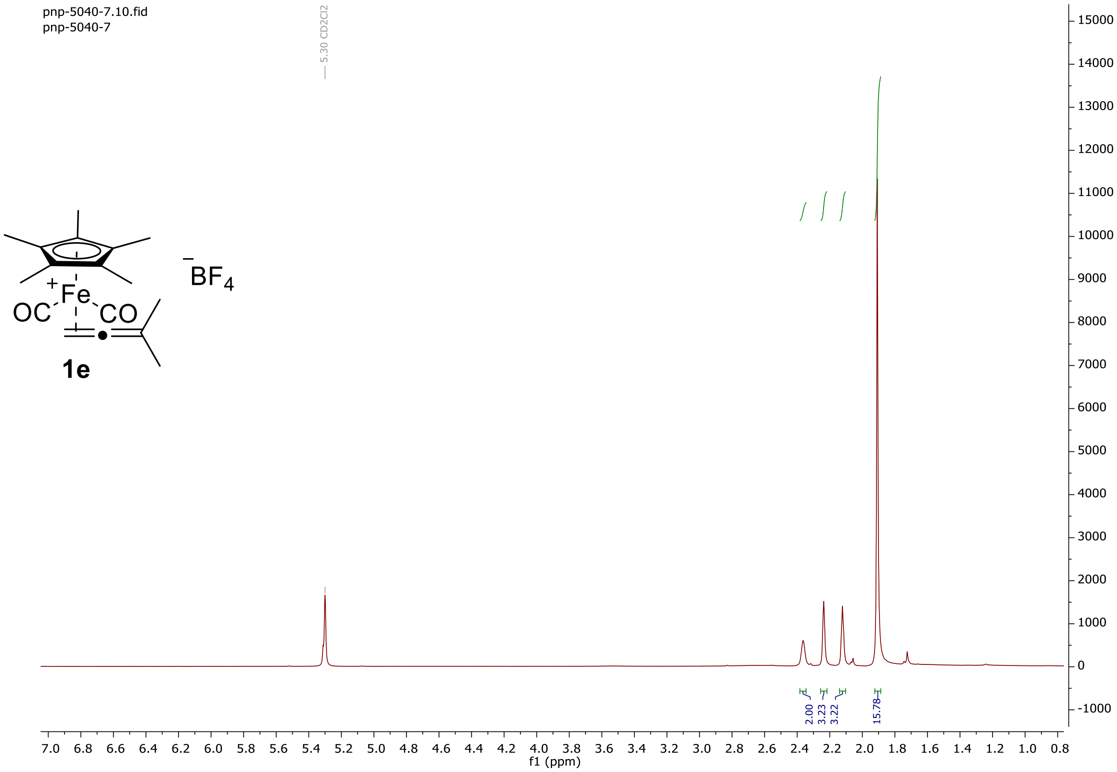
pnp-5040-7.10.fid
pnp-5040-7
5.30 CD2Cl2
1e
BF4
Fe
OC
CO
2.00
3.23
3.22
15.78
f1 (ppm)
7.0 6.8 6.6 6.4 6.2 6.0 5.8 5.6 5.4 5.2 5.0 4.8 4.6 4.4 4.2 4.0 3.8 3.6 3.4 3.2 3.0 2.8 2.6 2.4 2.2 2.0 1.8 1.6 1.4 1.2 1.0 0.8
15000 14000 13000 12000 11000 10000 9000 8000 7000 6000 5000 4000 3000 2000 1000 0 -1000

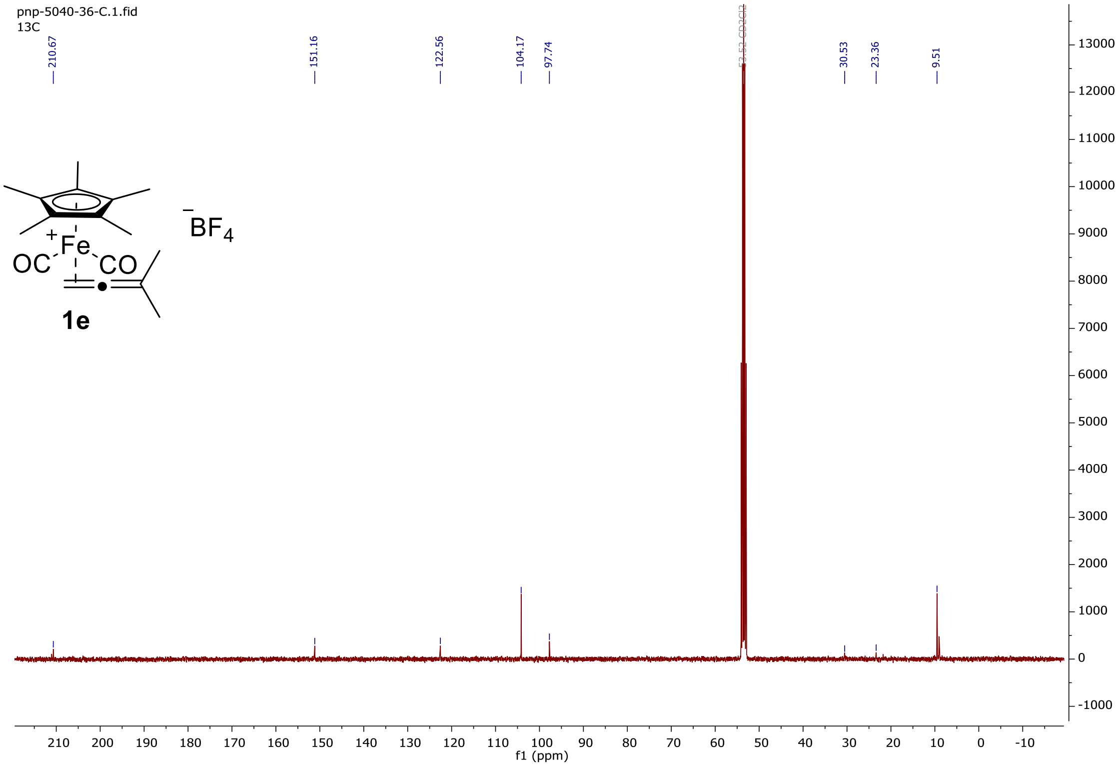
pnp-5040-36-C.1.fid
13C
210.67
151.16
122.56
104.17
97.74
53.53 CD2Cl2
30.53
23.36
9.51
Fe
OC
CO
BF4
1e
13000
12000
11000
10000
9000
8000
7000
6000
5000
4000
3000
2000
1000
0
-1000
210
200
190
180
170
160
150
140
130
120
110
100
90
80
70
60
50
40
30
20
10
0
-10
f1 (ppm)

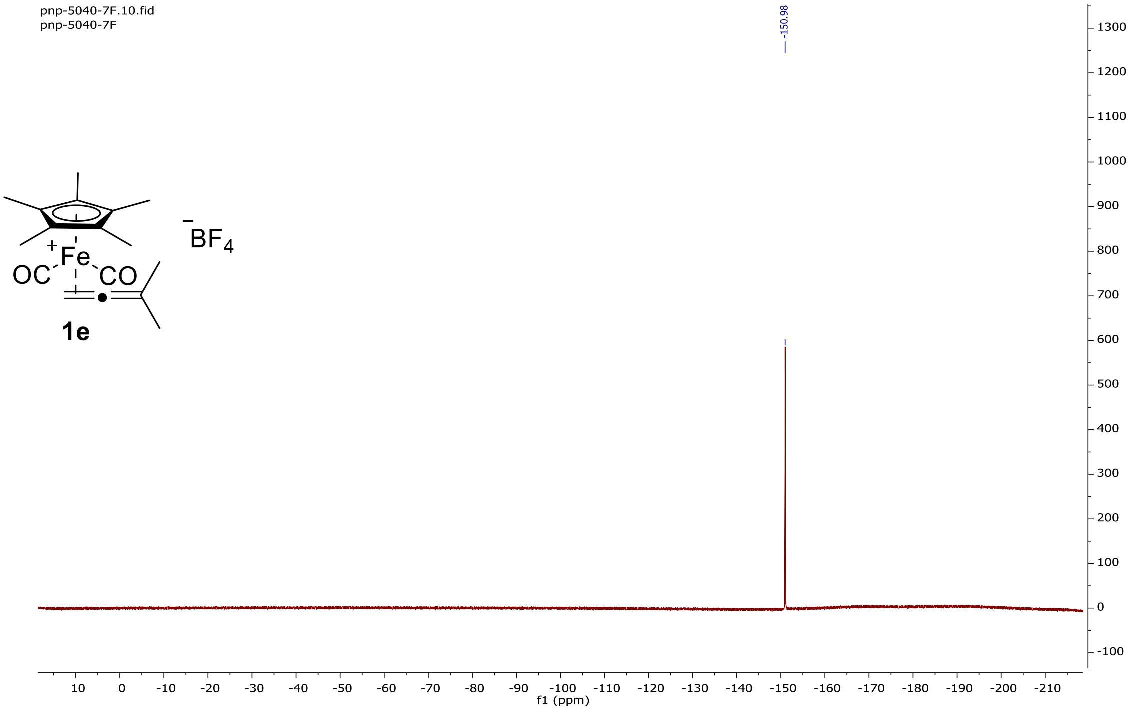
pnp-5040-7F.10.fid
pnp-5040-7F
-150.98
Fe
OC
CO
BF4
1e
1300
1200
1100
1000
900
800
700
600
500
400
300
200
100
0
-100
10
0
-10
-20
-30
-40
-50
-60
-70
-80
-90
-100
-110
-120
-130
-140
-150
-160
-170
-180
-190
-200
-210
f1 (ppm)

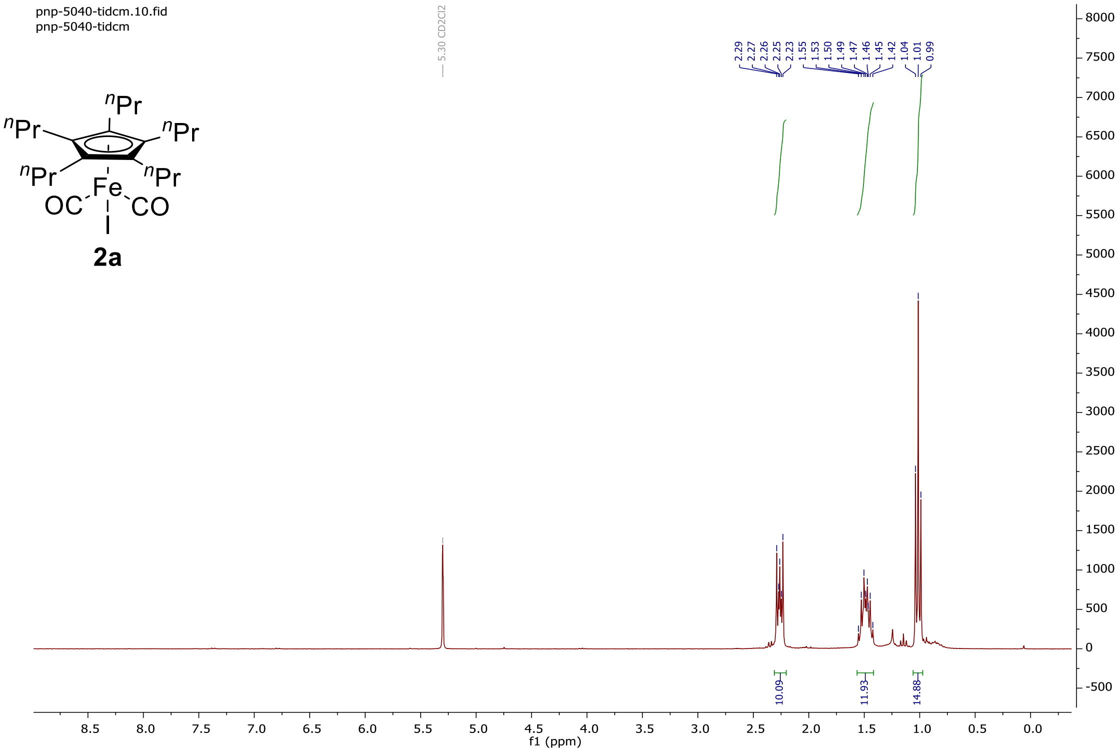
pnp-5040-tidcm.10.fid
pnp-5040-tidcm
5.30 CD2Cl2
2.29
2.27
2.26
2.25
2.23
1.55
1.53
1.50
1.49
1.47
1.46
1.45
1.42
1.04
1.01
0.99
10.09
11.93
14.88
^{n}Pr
Fe
OC
CO
I
2a
f1 (ppm)

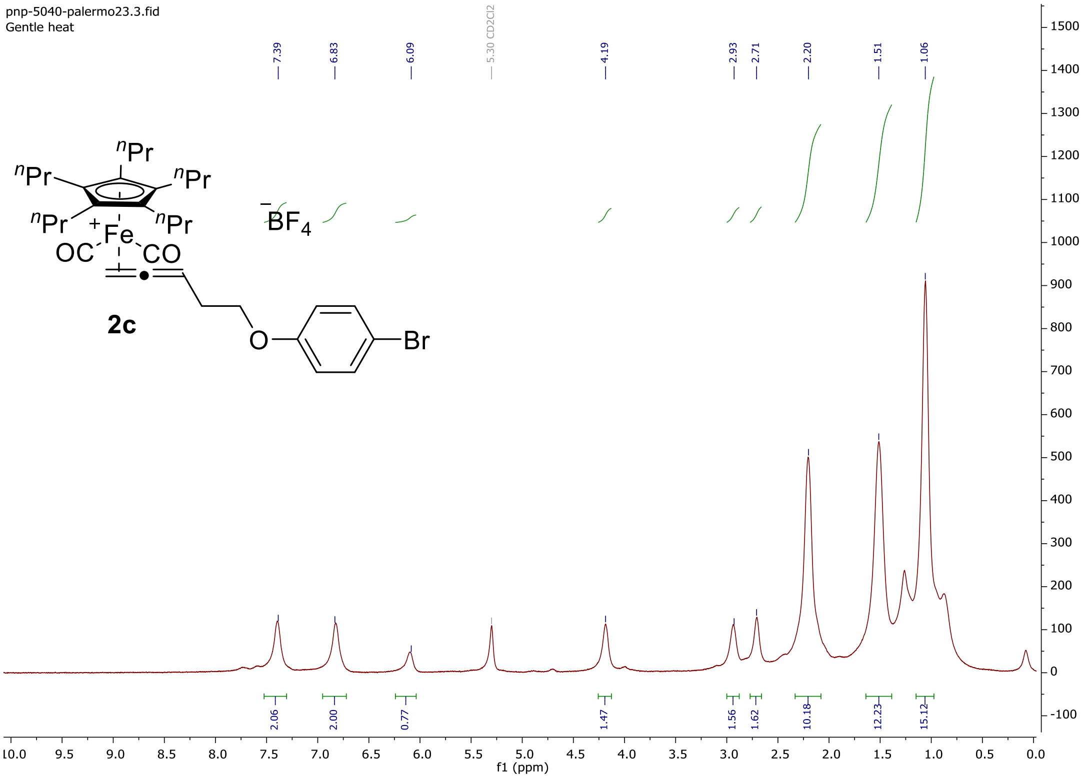
pnp-5040-palermo23.3.fid
Gentle heat
7.39
6.83
6.09
5.30 CD2Cl2
4.19
2.93
2.71
2.20
1.51
1.06
2.06
2.00
0.77
1.47
1.56
1.62
10.18
12.23
15.12
^{n}Pr
+Fe
OC
CO
$^-$BF$_4$
O
Br
2c
f1 (ppm)

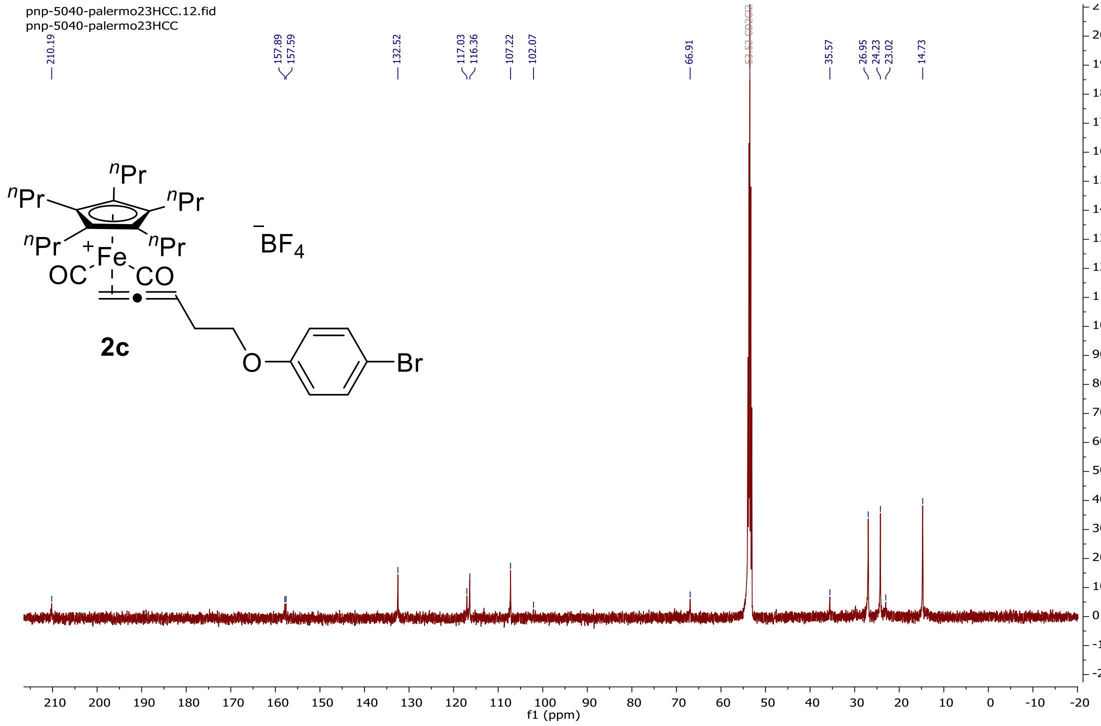
pnp-5040-palermo23HCC.12.fid
pnp-5040-palermo23HCC
210.19
157.89
157.59
132.52
117.03
116.36
107.22
102.07
66.91
53.52 CD2Cl2
35.57
26.95
24.23
23.02
14.73
nPr
nPr
nPr
nPr
nPr
+Fe
OC
CO
BF4
2c
O
Br
f1 (ppm)
210 200 190 180 170 160 150 140 130 120 110 100 90 80 70 60 50 40 30 20 10 0 -10 -20
2100 2000 1900 1800 1700 1600 1500 1400 1300 1200 1100 1000 900 800 700 600 500 400 300 200 100 0 -100 -200

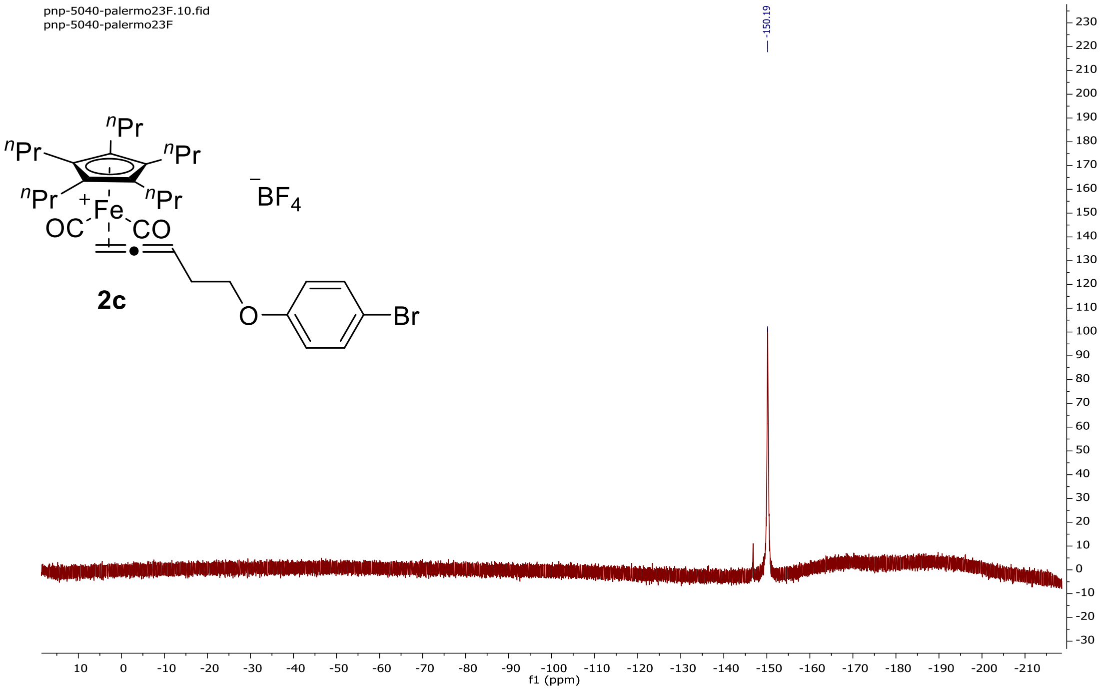
pnp-5040-palermo23F.10.fid
pnp-5040-palermo23F
-150.19
nPr
nPr
nPr
nPr
nPr
+Fe
OC
CO
BF4
2c
O
Br
f1 (ppm)
10 0 -10 -20 -30 -40 -50 -60 -70 -80 -90 -100 -110 -120 -130 -140 -150 -160 -170 -180 -190 -200 -210
230 220 210 200 190 180 170 160 150 140 130 120 110 100 90 80 70 60 50 40 30 20 10 0 -10 -20 -30

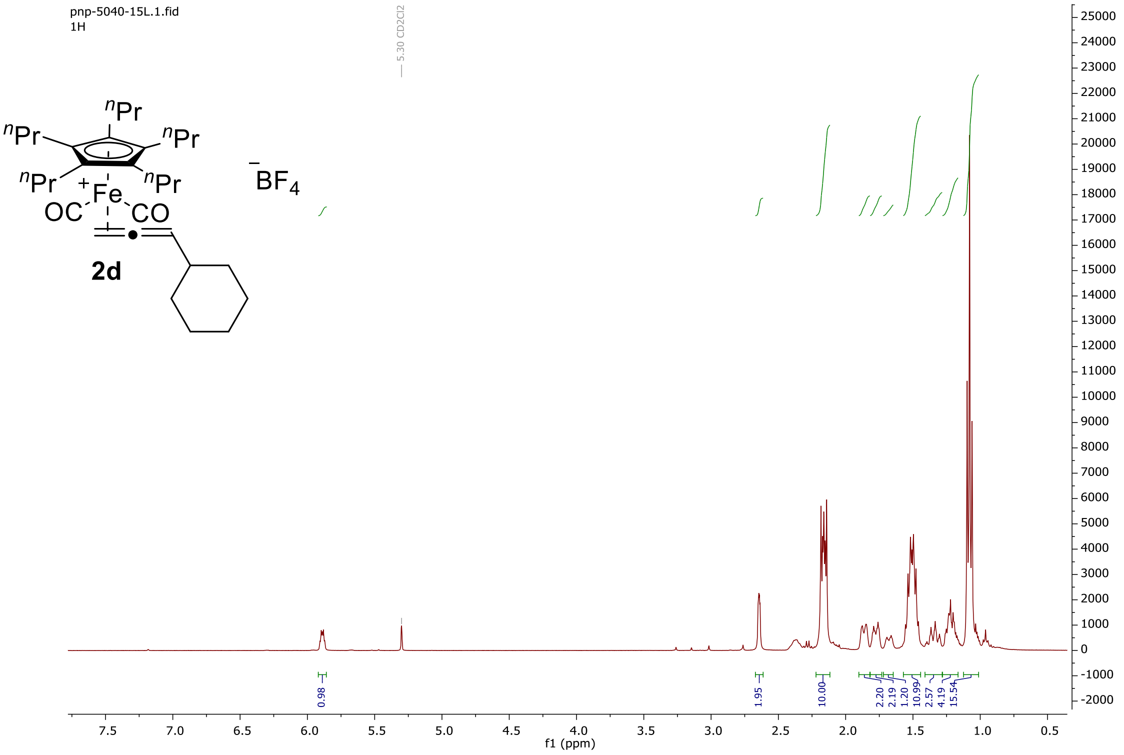
pnp-5040-15L.1.fid
1H
5.30 CD2Cl2
2d
nPr
+Fe
OC
CO
BF4
0.98
1.95
10.00
2.20
2.19
1.20
10.99
2.57
4.19
15.54
f1 (ppm)
7.5 7.0 6.5 6.0 5.5 5.0 4.5 4.0 3.5 3.0 2.5 2.0 1.5 1.0 0.5
25000 24000 23000 22000 21000 20000 19000 18000 17000 16000 15000 14000 13000 12000 11000 10000 9000 8000 7000 6000 5000 4000 3000 2000 1000 0 -1000 -2000

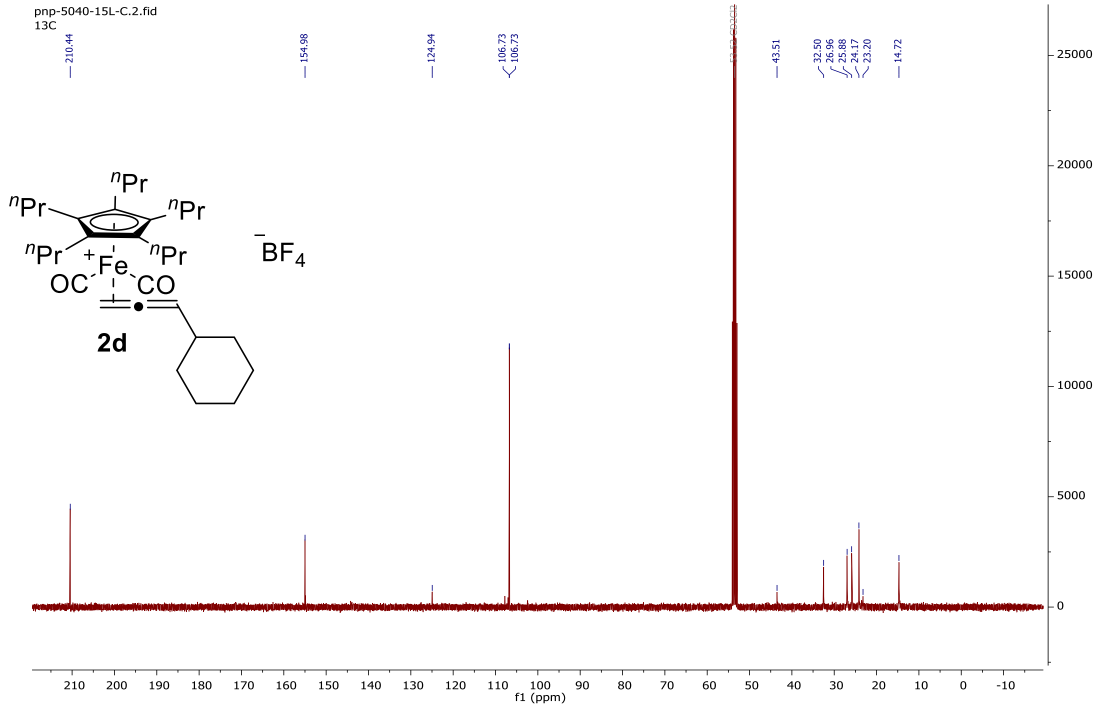
pnp-5040-15L-C.2.fid
13C
210.44
154.98
124.94
106.73
106.73
43.51
32.50
26.96
25.88
24.17
23.20
14.72
2d
nPr
+Fe
OC
CO
BF4
f1 (ppm)
210 200 190 180 170 160 150 140 130 120 110 100 90 80 70 60 50 40 30 20 10 0 -10
25000 20000 15000 10000 5000 0

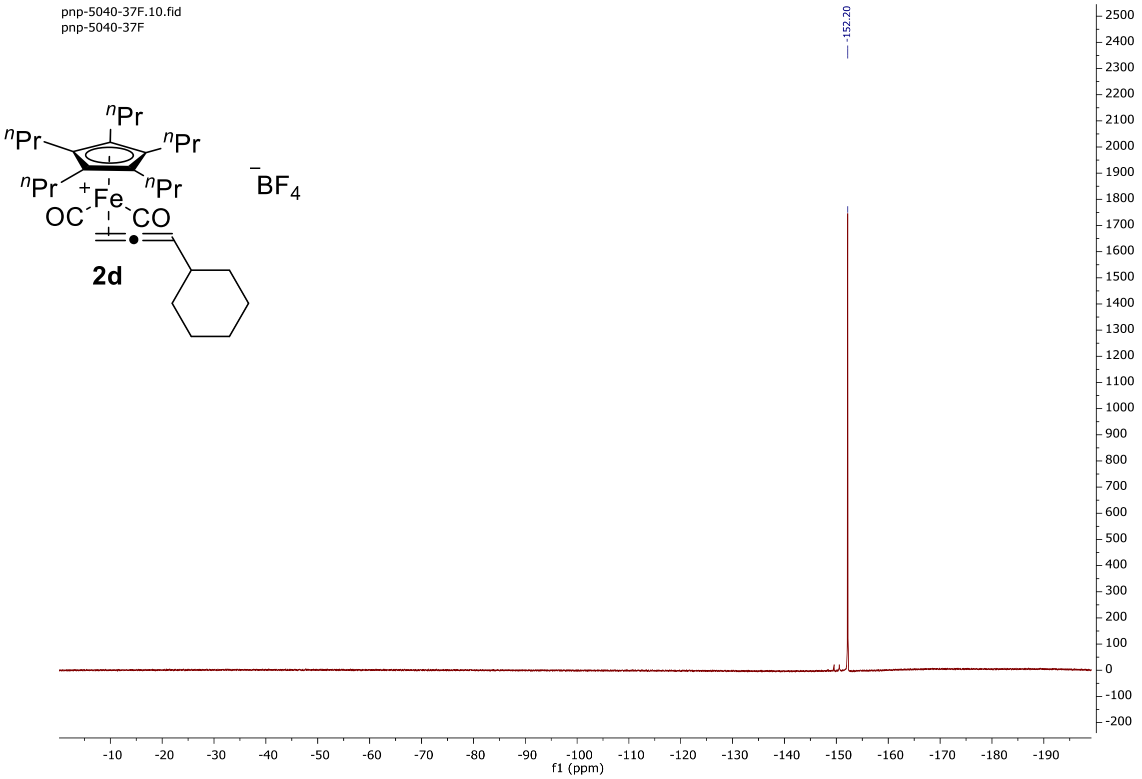
pnp-5040-37F.10.fid
pnp-5040-37F
-152.20
nPr
nPr
nPr
nPr
nPr
+Fe
OC
CO
BF4
2d
2500
2400
2300
2200
2100
2000
1900
1800
1700
1600
1500
1400
1300
1200
1100
1000
900
800
700
600
500
400
300
200
100
0
-100
-200
-10
-20
-30
-40
-50
-60
-70
-80
-90
-100
-110
-120
-130
-140
-150
-160
-170
-180
-190
f1 (ppm)

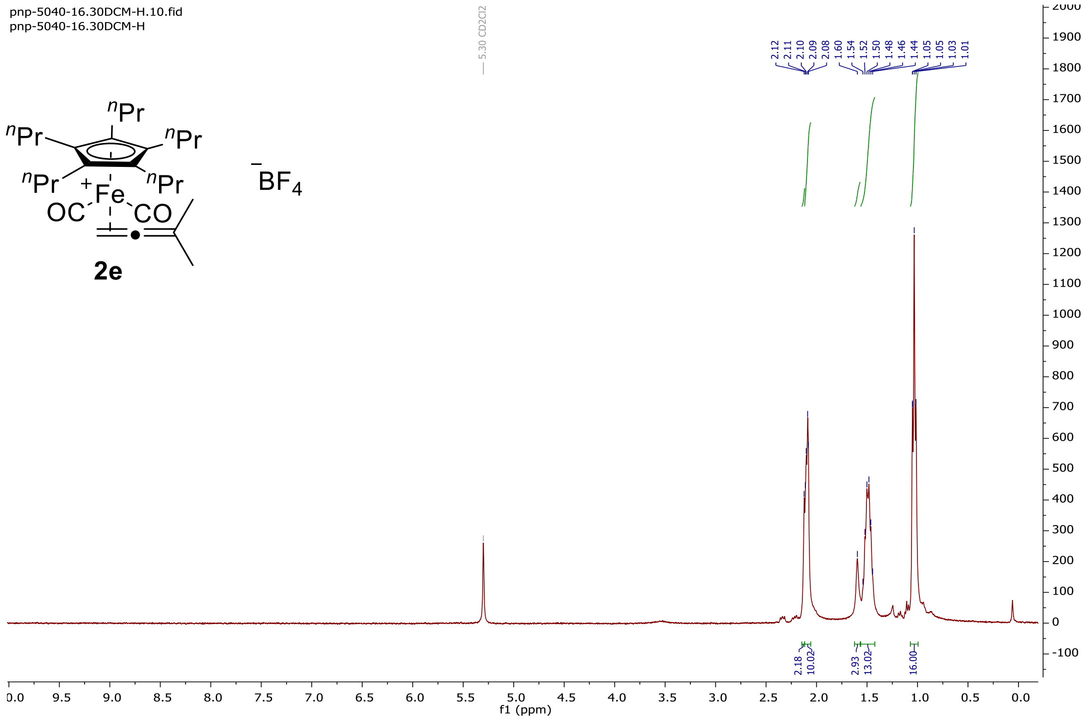
pnp-5040-16.30DCM-H.10.fid
pnp-5040-16.30DCM-H
5.30 CD2Cl2
2.12
2.11
2.10
2.09
2.08
1.60
1.54
1.52
1.50
1.48
1.46
1.44
1.05
1.05
1.03
1.01
nPr
nPr
nPr
nPr
nPr
+Fe
OC
CO
BF4
2e
2.18
10.02
2.93
13.02
16.00
2000
1900
1800
1700
1600
1500
1400
1300
1200
1100
1000
900
800
700
600
500
400
300
200
100
0
-100
0.0
9.5
9.0
8.5
8.0
7.5
7.0
6.5
6.0
5.5
5.0
4.5
4.0
3.5
3.0
2.5
2.0
1.5
1.0
0.5
0.0
f1 (ppm)

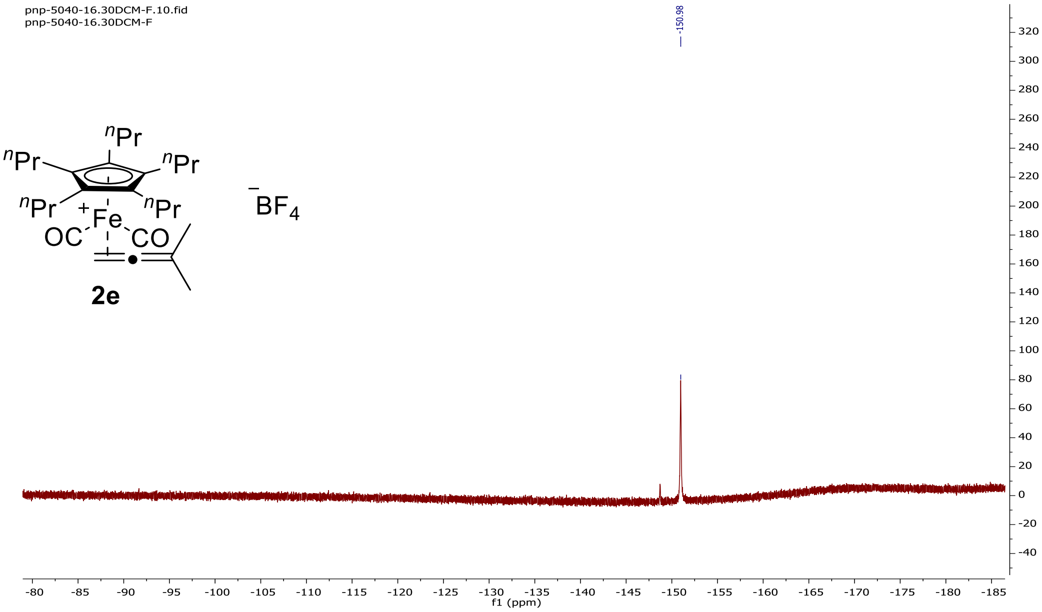
pnp-5040-16.30DCM-F.10.fid
pnp-5040-16.30DCM-F
-150.98
nPr
nPr
nPr
nPr
nPr
+Fe
OC
CO
BF4
2e
320
300
280
260
240
220
200
180
160
140
120
100
80
60
40
20
0
-20
-40
-80
-85
-90
-95
-100
-105
-110
-115
-120
-125
-130
-135
-140
-145
-150
-155
-160
-165
-170
-175
-180
-185
f1 (ppm)

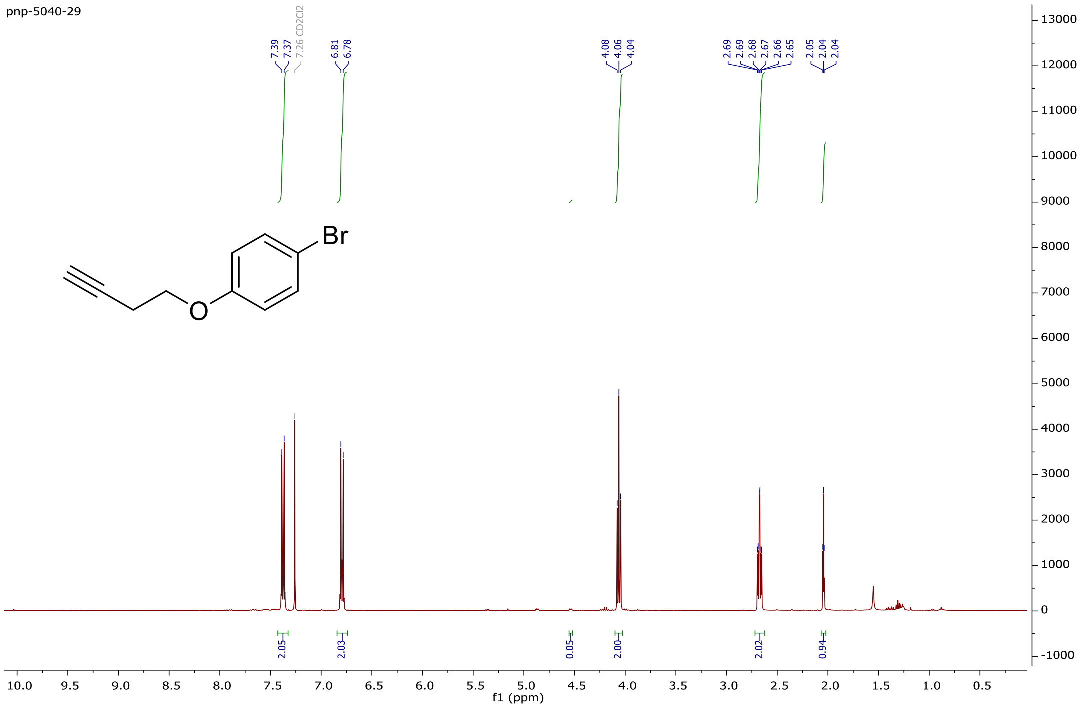
pnp-5040-29
7.39
7.37
7.26 CD2Cl2
6.81
6.78
4.08
4.06
4.04
2.69
2.69
2.68
2.67
2.66
2.65
2.05
2.04
2.04
Br
O
2.05
2.03
0.05
2.00
2.02
0.94
13000
12000
11000
10000
9000
8000
7000
6000
5000
4000
3000
2000
1000
0
-1000
10.0
9.5
9.0
8.5
8.0
7.5
7.0
6.5
6.0
5.5
5.0
4.5
4.0
3.5
3.0
2.5
2.0
1.5
1.0
0.5
f1 (ppm)

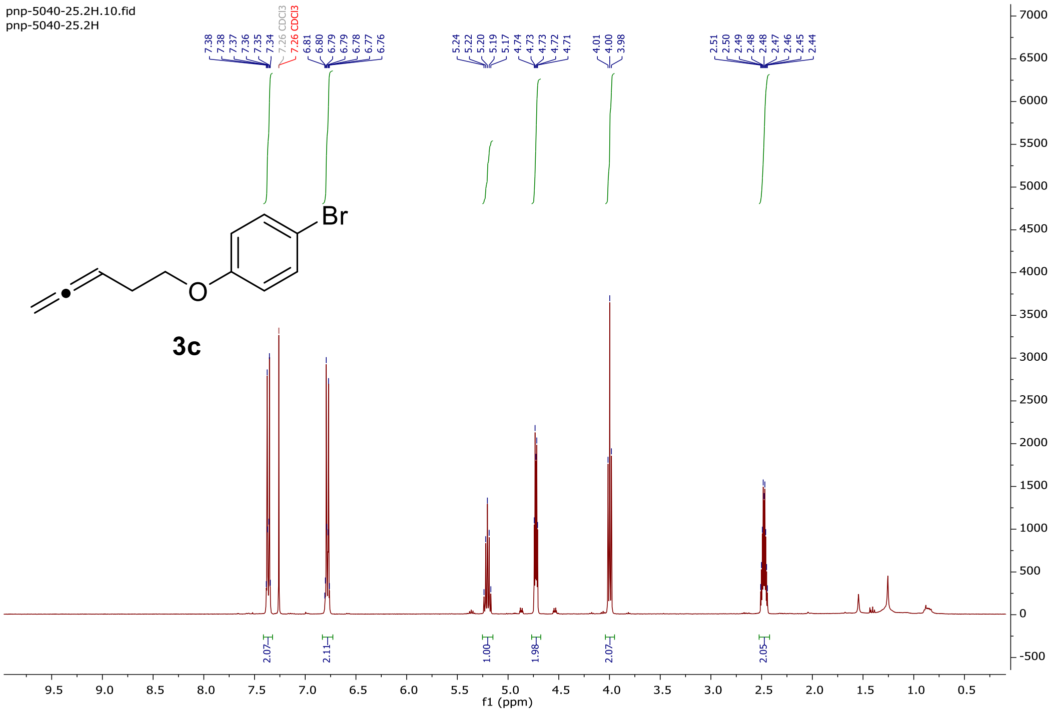
3c
pnp-5040-25.2H.10.fid
pnp-5040-25.2H
7.38 7.38 7.37 7.36 7.35 7.34 7.26 CDCl3 7.26 CDCl3 6.81 6.80 6.79 6.79 6.78 6.77 6.76
5.24 5.22 5.20 5.19 5.17 4.74 4.73 4.73 4.72 4.71 4.01 4.00 3.98
2.51 2.50 2.49 2.48 2.48 2.47 2.46 2.45 2.44
Br
O
2.07 2.11 1.00 1.98 2.07 2.05
f1 (ppm)
9.5 9.0 8.5 8.0 7.5 7.0 6.5 6.0 5.5 5.0 4.5 4.0 3.5 3.0 2.5 2.0 1.5 1.0 0.5
7000 6500 6000 5500 5000 4500 4000 3500 3000 2500 2000 1500 1000 500 0 -500

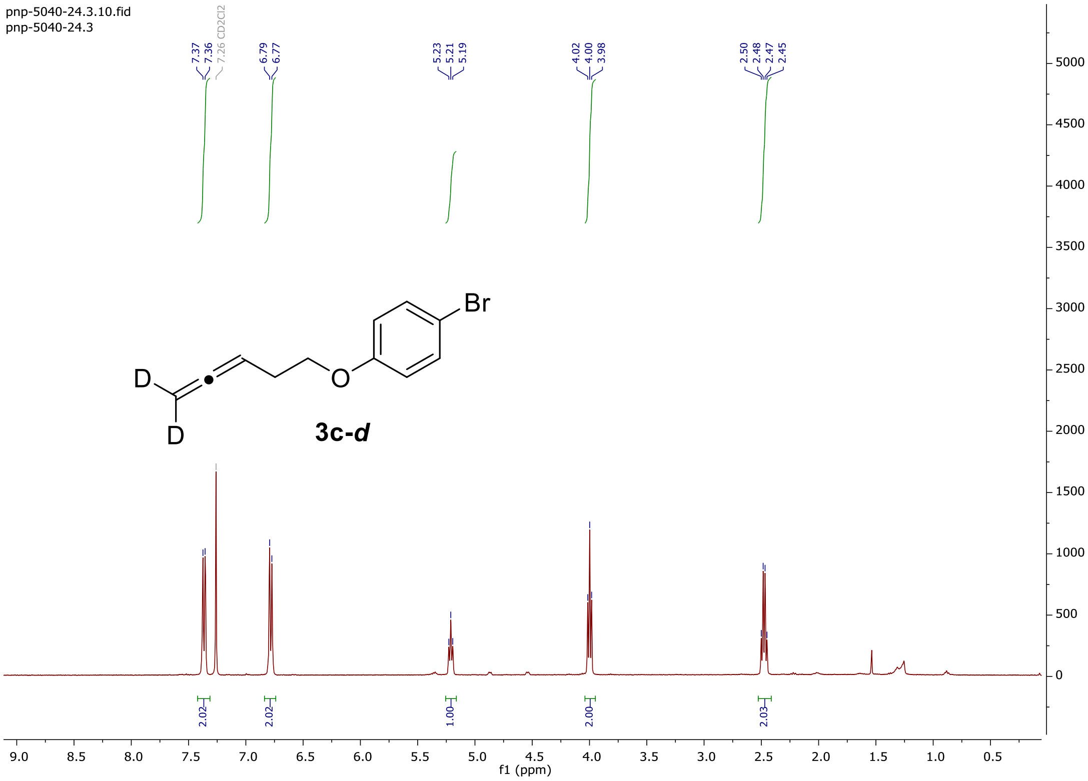
3c-*d*
pnp-5040-24.3.10.fid
pnp-5040-24.3
7.37 7.36 7.26 CD2Cl2 6.79 6.77
5.23 5.21 5.19
4.02 4.00 3.98
2.50 2.48 2.47 2.45
Br
O
D
D
2.02 2.02 1.00 2.00 2.03
f1 (ppm)
9.0 8.5 8.0 7.5 7.0 6.5 6.0 5.5 5.0 4.5 4.0 3.5 3.0 2.5 2.0 1.5 1.0 0.5
5000 4500 4000 3500 3000 2500 2000 1500 1000 500 0

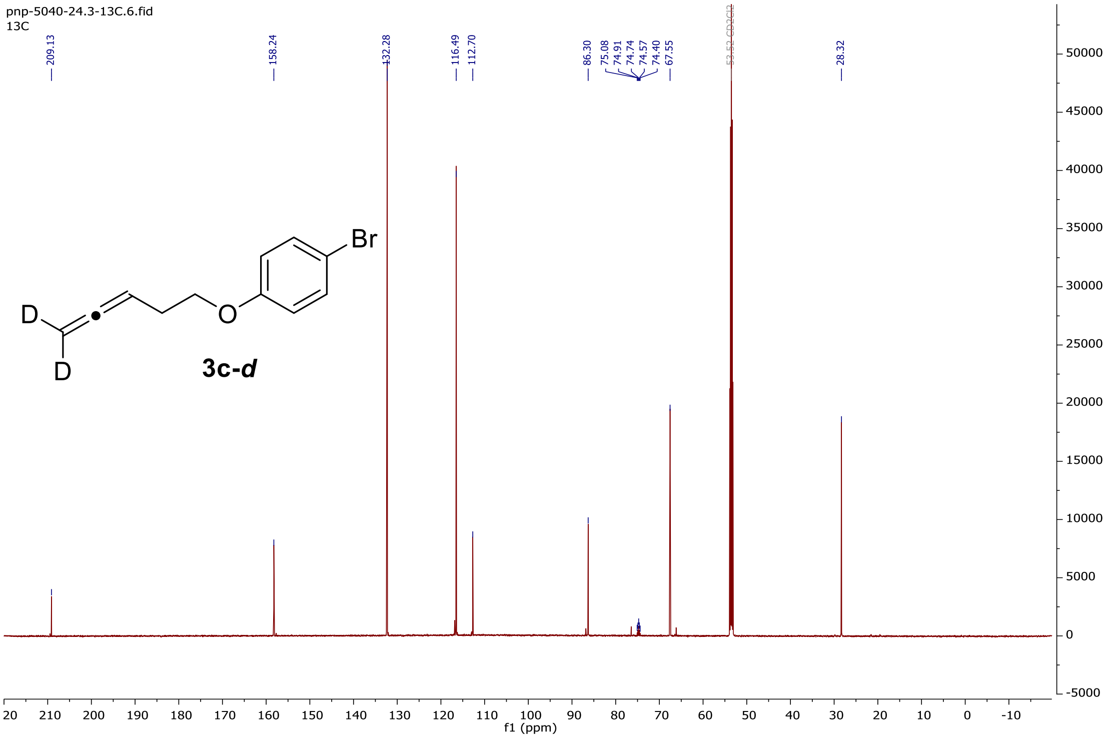
pnp-5040-24.3-13C.6.fid
13C
209.13
158.24
132.28
116.49
112.70
86.30
75.08
74.91
74.74
74.57
74.40
67.55
53.53 CD2Cl2
28.32
Br
O
D
D
3c-*d*
50000
45000
40000
35000
30000
25000
20000
15000
10000
5000
0
-5000
20
210
200
190
180
170
160
150
140
130
120
110
100
90
80
70
60
50
40
30
20
10
0
-10
f1 (ppm)

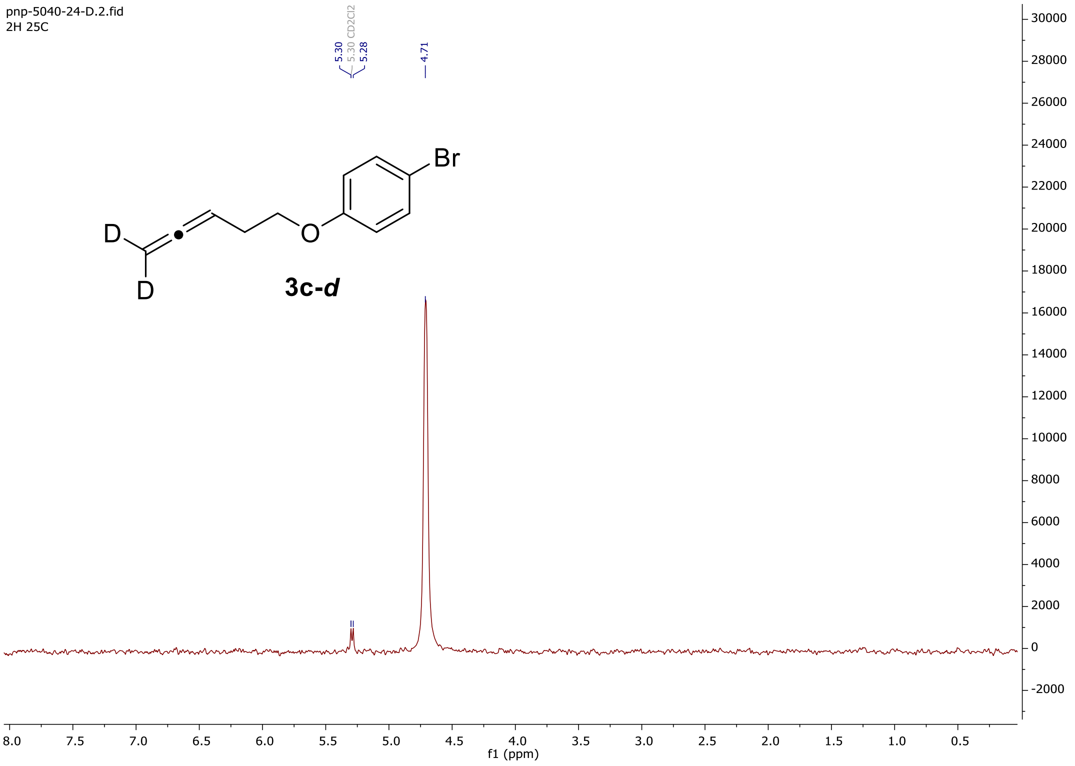
pnp-5040-24-D.2.fid
2H 25C
5.30
5.30 CD2Cl2
5.28
4.71
Br
O
D
D
3c-*d*
30000
28000
26000
24000
22000
20000
18000
16000
14000
12000
10000
8000
6000
4000
2000
0
-2000
8.0
7.5
7.0
6.5
6.0
5.5
5.0
4.5
4.0
3.5
3.0
2.5
2.0
1.5
1.0
0.5
f1 (ppm)

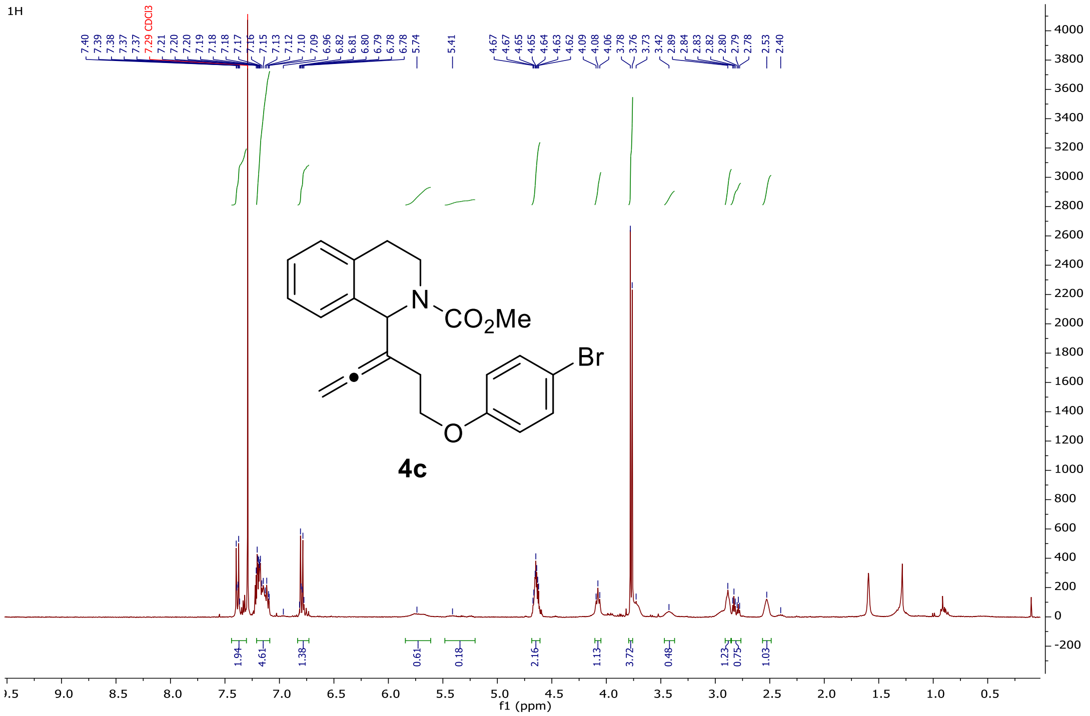
1H
7.40
7.39
7.38
7.37
7.37
7.29 CDCl3
7.21
7.20
7.20
7.19
7.18
7.18
7.17
7.16
7.15
7.13
7.12
7.10
7.09
6.96
6.82
6.81
6.80
6.79
6.78
6.78
5.74
5.41
4.67
4.67
4.65
4.65
4.64
4.63
4.62
4.09
4.08
4.06
3.78
3.76
3.73
3.42
2.89
2.84
2.83
2.82
2.80
2.79
2.78
2.53
2.40
N
CO$_2$Me
Br
O
4c
1.94
4.61
1.38
0.61
0.18
2.16
1.13
3.72
0.48
1.23
0.75
1.03
f1 (ppm)
4000
3800
3600
3400
3200
3000
2800
2600
2400
2200
2000
1800
1600
1400
1200
1000
800
600
400
200
0
-200

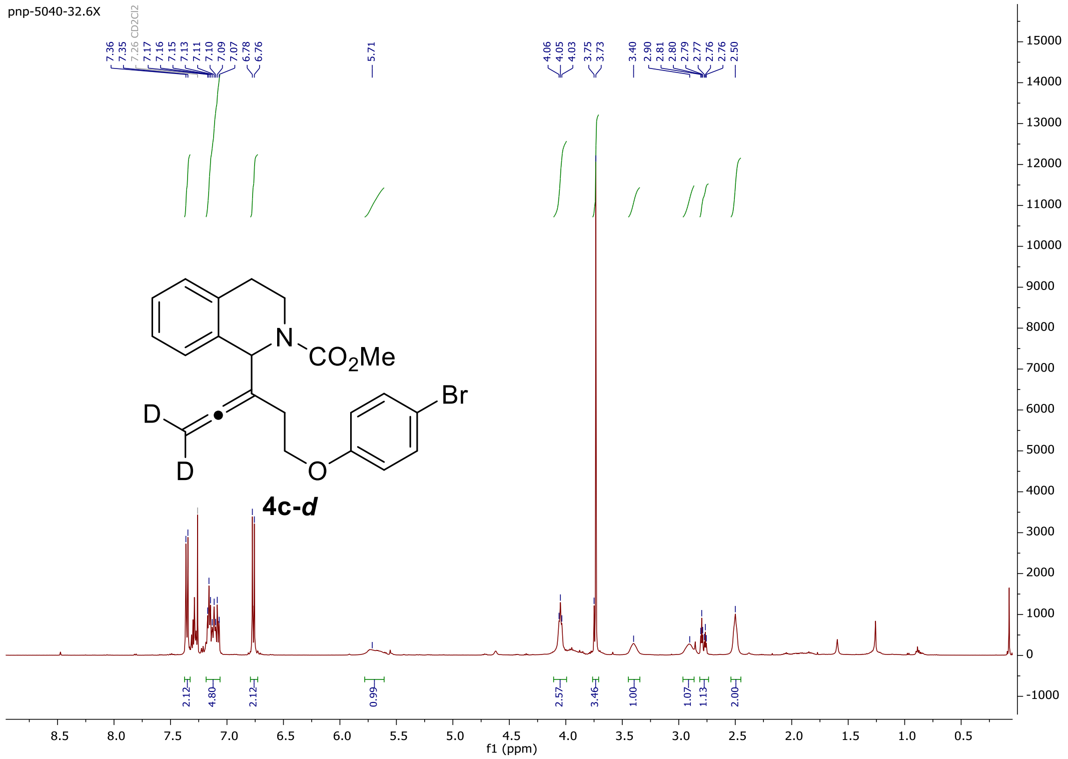
pnp-5040-32.6X
7.36
7.35
7.26 CD2Cl2
7.17
7.16
7.15
7.13
7.11
7.10
7.09
7.07
6.78
6.76
5.71
4.06
4.05
4.03
3.75
3.73
3.40
2.90
2.81
2.80
2.79
2.77
2.76
2.76
2.50
N
CO$_2$Me
Br
D
D
O
4c-*d*
2.12
4.80
2.12
0.99
2.57
3.46
1.00
1.07
1.13
2.00
f1 (ppm)
15000
14000
13000
12000
11000
10000
9000
8000
7000
6000
5000
4000
3000
2000
1000
0
-1000

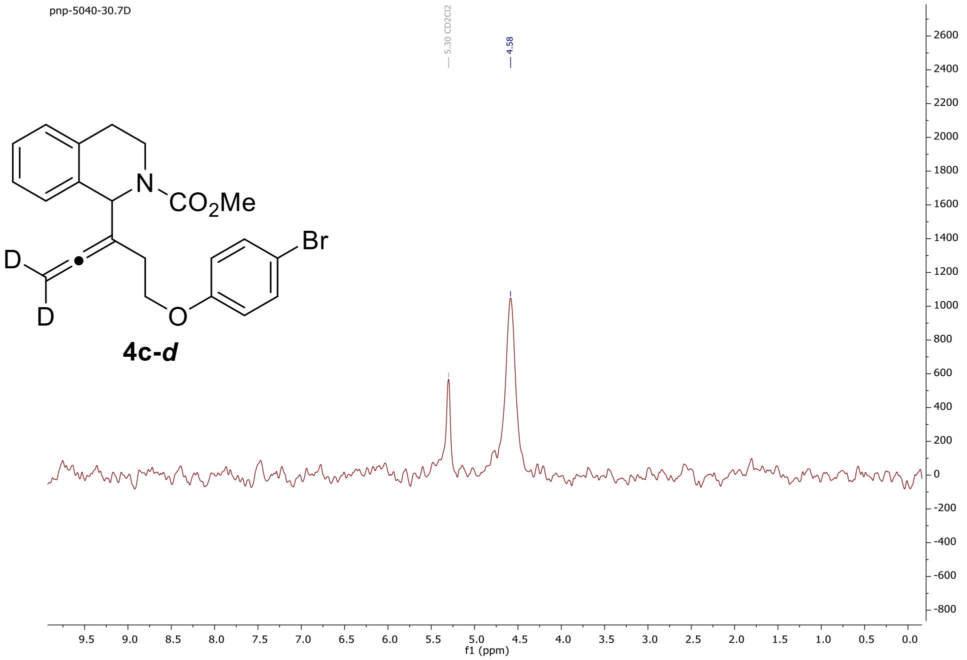
pnp-5040-30.7D
5.30 CD2Cl2
4.58
D
D
N
CO2Me
Br
O
2600
2400
2200
2000
1800
1600
1400
1200
1000
800
600
400
200
0
-200
-400
-600
-800
9.5 9.0 8.5 8.0 7.5 7.0 6.5 6.0 5.5 5.0 4.5 4.0 3.5 3.0 2.5 2.0 1.5 1.0 0.5 0.0
f1 (ppm)

4c-*d*

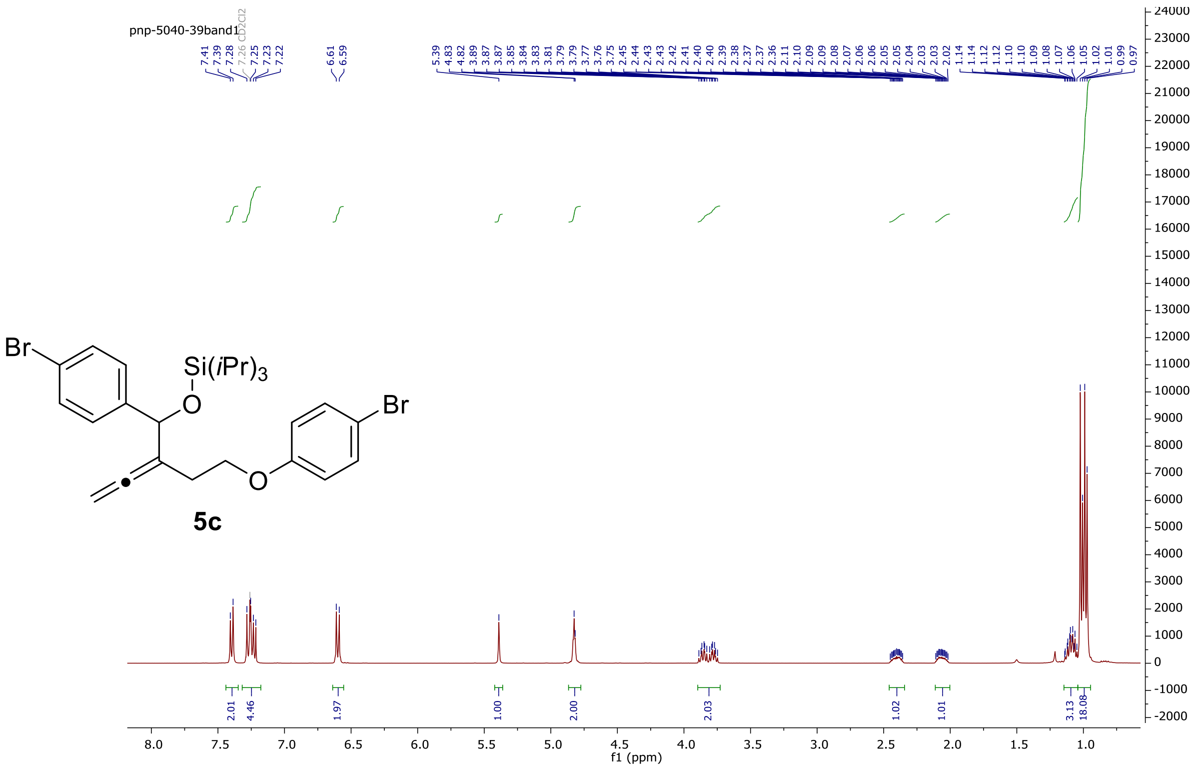
pnp-5040-39band1
7.41
7.39
7.28
7.26 CD2Cl2
7.25
7.23
7.22
6.61
6.59
5.39
4.83
4.82
3.89
3.87
3.87
3.85
3.84
3.83
3.81
3.79
3.79
3.77
3.76
3.75
2.45
2.44
2.43
2.43
2.42
2.41
2.40
2.39
2.38
2.37
2.37
2.36
2.11
2.10
2.09
2.09
2.08
2.07
2.06
2.06
2.05
2.05
2.04
2.03
2.03
2.02
1.14
1.12
1.12
1.10
1.10
1.09
1.08
1.07
1.06
1.05
1.02
1.01
0.99
0.97
Br
Si(iPr)3
O
Br
O
2.01
4.46
1.97
1.00
2.00
2.03
1.02
1.01
3.13
18.08
24000
23000
22000
21000
20000
19000
18000
17000
16000
15000
14000
13000
12000
11000
10000
9000
8000
7000
6000
5000
4000
3000
2000
1000
0
-1000
-2000
8.0 7.5 7.0 6.5 6.0 5.5 5.0 4.5 4.0 3.5 3.0 2.5 2.0 1.5 1.0
f1 (ppm)

5c

Appendix B : X-Ray Data

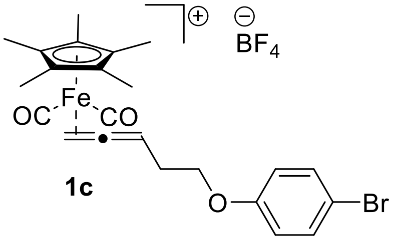

1c

Datablock: Palermo2a_a

```
Bond precision:  C-C = 0.0044 A          Wavelength=1.54178

Cell:            a=8.2960(4)     b=16.2677(8)        c=8.8173(4)
                 alpha=90        beta=90.059(2)      gamma=90
Temperature:     150 K

                Calculated                 Reported
Volume          1189.95(10)                1189.95(10)
Space group     P 21                       P 21
Hall group      P 2yb                      P 2yb
Moiety formula  C23 H26 Br Fe O3, B F4     ?
Sum formula     C23 H26 B Br F4 Fe O3      C23 H26 B Br F4 Fe O3
Mr              573.00                     573.01
Dx,g cm-3       1.599                      1.599
Z               2                          2
Mu (mm-1)       7.535                      7.535
F000            580.0                      580.0
F000'           578.11
h,k,lmax        9,19,10                    9,19,10
Nref            4373[ 2269]                4107
Tmin,Tmax       0.731,0.942                0.500,0.750
Tmin'           0.265

Correction method= # Reported T Limits: Tmin=0.500 Tmax=0.750
AbsCorr = MULTI-SCAN

Data completeness= 1.81/0.94       Theta(max)= 68.296

R(reflections)= 0.0205( 3973)      wR2(reflections)= 0.0571( 4107)

S = 0.640                   Npar= 315
```

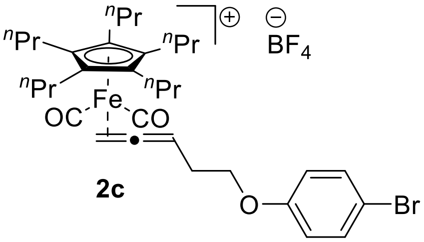

2c

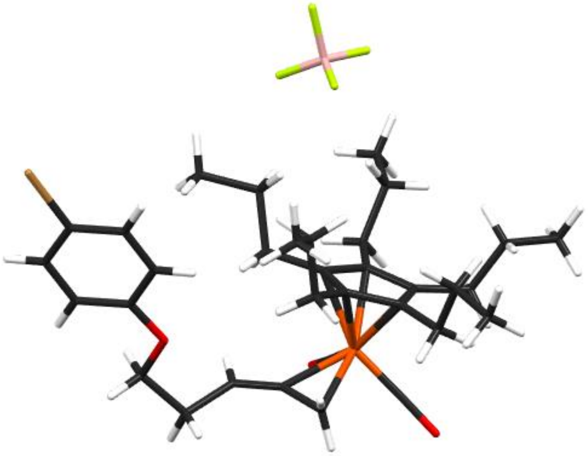

Datablock: palermo25_0m_a

```
Bond precision:    C-C = 0.0066 A          Wavelength=1.54178

Cell:              a=12.0793(3)       b=12.1237(3)       c=14.0632(3)
                   alpha=65.325(2)    beta=81.066(2)     gamma=67.243(2)
Temperature:       100 K

                   Calculated                    Reported
Volume             1725.71(8)                    1725.71(8)
Space group        P -1                          P -1
Hall group         -P 1                          -P 1
Moiety formula     C33 H46 Br Fe O3, B F4        C33 H46 Br Fe O3, B F4
Sum formula        C33 H46 B Br F4 Fe O3         C34 H49 B Br F4 Fe O3
Mr                 713.26                        728.30
Dx,g cm-3          1.373                         1.402
Z                  2                             2
Mu (mm-1)          5.301                         5.312
F000               740.0                         758.0
F000'              738.44
h,k,lmax           14,14,16                      14,14,16
Nref               6348                          6189
Tmin,Tmax          0.974,0.974                   0.439,0.753
Tmin'              0.974

Correction method= # Reported T Limits: Tmin=0.439 Tmax=0.753
AbsCorr = MULTI-SCAN

Data completeness= 0.975             Theta(max)= 68.419

                                                 wR2(reflections)=
R(reflections)= 0.0531( 4939)                    0.1429( 6189)

S = 1.038                    Npar= 393
```

Bibliography

(1) Wilkinson, G.; Rosenblum, M.; Whiting, M. C.; Woodward, R. B. THE STRUCTURE OF IRON BIS-CYCLOPENTADIENYL. *Journal of the American Chemical Society* **1952**, *74* (8), 2125-2126. DOI: 10.1021/ja01128a527.

(2) Bibler, J. P.; Wojcicki, A. Reactions of Cyclopentadienyl (methyl) iron Dicarbonyl with Various Ligands. Cyclopentadienyl(acetyl)iron Carbonyl Phosphine and Phosphite Complexes. *Inorganic Chemistry* **1966**, *5* (5), 889-892. DOI: 10.1021/ic50039a037.

(3) Giering, W. P.; Rosenblum, M. Metal-assisted cycloaddition reactions. *Journal of the American Chemical Society* **1971**, *93* (20), 5299-5301. DOI: 10.1021/ja00749a079.

(4) Giering, W. P.; Raghu, S.; Rosenblum, M.; Cutler, A.; Ehtholt, D.; Fish, R. W. Synthesis of .gamma.-lactams and sultams by metal assisted cycloaddition. Stereochemistry of cycloaddition and of the deprotonation of cationic pentahaptocyclopentadienyldicaronyl(olefin)iron complexes. *Journal of the American Chemical Society* **1972**, *94* (23), 8251-8253. DOI: 10.1021/ja00778a063.

(5) Raghu, S.; Rosenblum, M. Metal assisted cycloaddition reactions of dicarbonyl(pentahaptocylopentadienyl)(allenyl)iron. Mechanism and synthetic applications. Stereospecificity of protonation of dicarbonyl(pentahaptocyclopentadienyl)(propargyl)iron. *Journal of the American Chemical Society* **1973**, *95* (9), 3060-3062. DOI: 10.1021/ja00790a079.

(6) Lichtenberg, D. W.; Wojcicki, A. Reactions of coordinated propargyl and allene ligands in cyclopentadienyliron dicarbonyl complexes. *Journal of Organometallic Chemistry* **1975**, *94* (2), 311-326. DOI: 10.1016/s0022-328x(00)88726-4 (acccessed 2022-04-04T18:49:34).

(7) Celebuski, J.; Rosenblum, M. Carbon-carbon bond formation employing organoiron reagents. *Tetrahedron* **1985**, *41* (24), 5741-5746. DOI: 10.1016/s0040-4020(01)91411-5 (acccessed 2022-04-05T18:07:28).

(8) Cardoso, J. M. S.; Fernandes, A.; Cardoso, B. d. P.; Carvalho, M. D.; Ferreira, L. P.; Calhorda, M. J.; Royo, B. Cationic Half-Sandwich Iron(II) and Iron(III) Complexes with N-Heterocyclic Carbene Ligands. *Organometallics* **2014**, *33* (20), 5670-5677. DOI: 10.1021/om500528p.

(9) Fukumoto, K.; Sakai, A.; Hayasaka, K.; Nakazawa, H. Desulfurization and H-Migration of Secondary Thioamides Catalyzed by an Iron Complex to Yield Imines and Their Reaction Mechanism. *Organometallics* **2013**, *32* (10), 2889-2892. DOI: 10.1021/om400304v.

(10) Knölker, H.-J.; Baum, E.; Goesmann, H.; Klauss, R. Demetalation of Tricarbonyl(cyclopentadienone)iron Complexes Initiated by a Ligand Exchange Reaction with NaOH—X-Ray Analysis of a Complex with Nearly Square-Planar Coordinated Sodium. *Angewandte Chemie International Edition* **1999**, *38* (13-14), 2064-2066, https://doi.org/10.1002/(SICI)1521-3773(19990712)38:13/14<2064::AID-ANIE2064>3.0.CO;2-W. DOI: https://doi.org/10.1002/(SICI)1521-3773(19990712)38:13/14<2064::AID-ANIE2064>3.0.CO;2-W (acccessed 2022/04/04).

(11) Hatanaka, T.; Ohki, Y.; Tatsumi, K. C□H Bond Activation/Borylation of Furans and Thiophenes Catalyzed by a Half-Sandwich Iron N-Heterocyclic Carbene Complex. *Chemistry - An Asian Journal* **2010**, *5* (7), 1657-1666. DOI: 10.1002/asia.201000140 (acccessed 2022-04-04T19:50:07).

(12) Hirsch, S. S.; Bailey, W. J. Base-catalyzed alkylation of cyclopentadiene rings with alcohols and amines. *The Journal of Organic Chemistry* **1978**, *43* (21), 4090-4094. DOI: 10.1021/jo00415a022.

(13) Csáky, A. G.; Contreras, C.; Mba, M.; Plumet, J. Regioselective Synthesis of Trisubstituted Cyclopentadienyl Ligands from Furans. *Synlett* **2002**, *2002* (09), 1451-1454. DOI: 10.1055/s-2002-34148.

(14) Venier, C. G.; Casserly, E. W. Di-tert-butylcyclopentadiene and tri-tert-butylcyclopentadiene. *Journal of the American Chemical Society* **1990**, *112* (7), 2808-2809. DOI: 10.1021/ja00163a057.

(15) Alonso, M.; Herradón, B. Substituent effects on the aromaticity of carbocyclic five-membered rings. *Phys. Chem. Chem. Phys.* **2010**, *12* (6), 1305-1317. DOI: 10.1039/b917343a (acccessed 2023-01-25T17:50:38).

(16) Calabro, D. C.; Hubbard, J. L.; Blevins, C. H., II; Campbell, A. C.; Lichtenberger, D. L. Effects of methyl group substitution on metal-coordinated cyclopentadienyl rings. Core and valence ionizations of methylated tricarbonyl(.eta.5-cyclopentadienyl)metal complexes. *Journal of the American Chemical Society* **1981**, *103* (23), 6839-6846. DOI: 10.1021/ja00413a010.

(17) Thompson, M. E., Bercaw, J.E. Some aspects of the chemistry of alkyl and hydride derivatives of permethylscandocene. Pure and Applied Chemistry, 1984; Vol. 56, pp 1–11.

(18) Robbins, J. L.; Edelstein, N. M.; Cooper, S. R.; Smart, J. C. Syntheses and electronic structures of decamethylmanganocenes. *Journal of the American Chemical Society* **1979**, *101* (14), 3853-3857. DOI: 10.1021/ja00508a023.

(19) Thornberry, M. P.; Slebodnick, C.; Deck, P. A.; Fronczek, F. R. Structural and Electronic Effects of Pentafluorophenyl Substituents on Cyclopentadienyl Complexes of Fe, Co, Mn, and Re1. *Organometallics* **2000**, *19* (25), 5352-5369. DOI: 10.1021/om000798v.

(20) Wang, Y.; Zhu, J.; Durham, A. C.; Lindberg, H.; Wang, Y.-M. α-C–H Functionalization of π-Bonds Using Iron Complexes: Catalytic Hydroxyalkylation of Alkynes and Alkenes. *Journal of the American Chemical Society* **2019**, *141* (50), 19594-19599. DOI: 10.1021/jacs.9b11716.

(21) Wang, Y.; Scrivener, S. G.; Zuo, X.-D.; Wang, R.; Palermo, P. N.; Murphy, E.; Durham, A. C.; Wang, Y.-M. Iron-Catalyzed Contrasteric Functionalization of Allenic C(sp2)–H Bonds: Synthesis of α-Aminoalkyl 1,1-Disubstituted Allenes. *Journal of the American Chemical Society* **2021**, *143* (37), 14998-15004. DOI: 10.1021/jacs.1c07512.

(22) Xia, Y.; Wade, N. W.; Palermo, P. N.; Wang, Y.; Wang, Y.-M. Contrasteric coupling of allenes and tetrahydroisoquinolines by iron-catalysed allenic C(sp2)–H functionalisation. *Chemical Communications* **2021**, *57* (98), 13329-13332, 10.1039/D1CC05949A. DOI: 10.1039/D1CC05949A.

(23) Kondo, M.; Omori, M.; Hatanaka, T.; Funahashi, Y.; Nakamura, S. Catalytic Enantioselective Reaction of Allenylnitriles with Imines Using Chiral Bis(imidazoline)s Palladium(II) Pincer Complexes. *Angewandte Chemie International Edition* **2017**, *56* (30), 8677-8680, https://doi.org/10.1002/anie.201702429. DOI: https://doi.org/10.1002/anie.201702429 (acccessed 2023/02/27).

(24) Mbofana, C. T.; Miller, S. J. Diastereo- and Enantioselective Addition of Anilide-Functionalized Allenoates to N-Acylimines Catalyzed by a Pyridylalanine-Based Peptide. *Journal of the American Chemical Society* **2014**, *136* (8), 3285-3292. DOI: 10.1021/ja412996f.

(25) Michelot, D.; Clinet, J.-C.; Linstrumelle, G. Allenyllithium Reagents (VI)1. A Highly Regioselective Metalation of Allenic Hydrocarbons2. A Route to Mono, DI, TRI or Tetrasubstituted Allenes. *Synthetic Communications* **1982**, *12* (10), 739-747. DOI: 10.1080/00397918208061912.

(26) Chakraborty, U.; Modl, M.; Mühldorf, B.; Bodensteiner, M.; Demeshko, S.; van Velzen, N. J. C.; Scheer, M.; Harder, S.; Wolf, R. Pentaarylcyclopentadienyl Iron, Cobalt, and Nickel Halides. *Inorganic Chemistry* **2016**, *55* (6), 3065-3074. DOI: 10.1021/acs.inorgchem.5b02896.

(27) Turner, J.; Chilton, N. F.; Kumar, A.; Colebatch, A. L.; Whittell, G. R.; Sparkes, H. A.; Weller, A. S.; Manners, I. Iron Precatalysts with Bulky Tri(tert-butyl)cyclopentadienyl Ligands for the Dehydrocoupling of Dimethylamine-Borane. *Chemistry – A European Journal* **2018**, *24* (53), 14127-14136, https://doi.org/10.1002/chem.201705316. DOI: https://doi.org/10.1002/chem.201705316 (acccessed 2023/02/28).

(28) Ding, R.; Wang, Y.; Wang, Y.-M. Synthesis of 1,1-Disubstituted Allenylic Silyl Ethers through Iron-Catalyzed Regioselective C(sp2)–H Functionalization of Allenes. *Synthesis* **2023**, *55* (05), 733-743. DOI: 10.1055/a-2004-0951.

(29) Natarajan, M.; Li, X.; Zhong, W.; Wang, W.; Xiao, Z.; Jiang, X.; Lu, C.; Liu, X. Three half-sandwiched iron(II) monocarbonyl complexes with PNP ligands: Their chemistry upon reduction and catalysis on proton reduction. *Electrochimica Acta* **2022**, *433*, 141207. DOI: https://doi.org/10.1016/j.electacta.2022.141207.

(30) Behrendt, U.; Pfeifer, R.-M.; Wartchow, R.; Butenschön, H. Some bimetallic half sandwich iron complexes with metal carbene substitution at the cyclopentadienyl ligand: synthesis,

characterization, structure, and cyclic voltammetry. *New Journal of Chemistry* **1999**, *23* (8), 891-895, 10.1039/A902815C. DOI: 10.1039/A902815C.